

Development of an engineered probiotic for the treatment of branched chain amino acid related metabolic diseases

Ning Li (✉ fromningli@gmail.com)

Synlogic Inc

Alex Tucker

Ginkgo Bioworks

Jian-Rong Gao

Synlogic

Lauren Renaud

Synlogic Inc

Michael James

Synlogic

Mary Castillo

Synlogic Inc.

Silvia Galvan

Ginkgo Bioworks

Rishi Jain

Ginkgo Bioworks

Ryan Putman

Ginkgo Bioworks

Scott Marr

Ginkgo Bioworks

Dylan Carlin

Ginkgo Bioworks

Kolea Zimmerman

Ginkgo Bioworks

Laura Stone

DSM Biotechnology Center, Delft, The Netherlands <https://orcid.org/0000-0001-9410-8220>

Christopher Bergeron

Synlogic

Mylene Perreault

Synlogic Inc

Patrick Boyle

Ginkgo Bioworks

Caroline Kurtz

Synlogic Inc <https://orcid.org/0000-0001-7192-6116>

Article

Keywords: branched chain amino acid (BCAA), metabolic dysfunction, metabolic diseases

Posted Date: March 16th, 2021

DOI: <https://doi.org/10.21203/rs.3.rs-318620/v1>

License:   This work is licensed under a Creative Commons Attribution 4.0 International License.

[Read Full License](#)

Development of an Engineered Microbe for the Treatment of Branched Chain Amino Acid Related Metabolic Diseases

Ning Li^{1*}†, Alex Tucker²†, JR Gao¹, Lauren Renaud¹, Michael James¹, Mary Joan Castillo¹, Silvia Galvan², Rishi Jain², Ryan Putman², Scott Marr², Dylan Alexander Carlin², Kolea Zimmerman², Laura K. Stone², Chris Bergeron¹, Mylene Perreault¹, Patrick Boyle², Caroline Kurtz^{1*}

¹Synlogic Inc., Cambridge, Massachusetts, USA

²Ginkgo Bioworks, Boston, USA

†Equal contribution

*Correspondence to Ning Li fromningli@gmail.com, Caroline Kurtz caroline@synlogictx.com

1 **Abstract**

2 Metabolic dysfunction arising from missing or impaired enzymes comprising the
3 branched chain amino acid (BCAA) degradation pathway, especially those involving
4 leucine, can result in the accumulation of toxic metabolic intermediates and cause
5 severe metabolic disease. Removal of dietary BCAAs via their degradation by
6 engineered microbes could be a viable approach to prevent BCAA-mediated disease
7 sequelae. In this article, we describe the design and construction of an engineered
8 leucine degrading strain of *E. coli* Nissle 1917, the improvement of the degradation
9 pathway through high throughput screening, and the demonstration of strain activity in
10 animal models monitored by disease and strain-specific biomarkers. This work provides
11 a path for the development of engineered probiotic bacterial strains as a treatment for
12 BCAA-related metabolic diseases and disorders in humans.

13 **Introduction**

14 Human proteins are comprised of 20 amino acids, 9 of which are deemed essential
15 because they cannot be synthesized by the human body. Essential amino acids must
16 therefore be obtained from the diet. The branched-chain amino acids (BCAAs) leucine
17 (Leu), isoleucine, and valine belong to this group[1]. BCAAs are reported to promote
18 protein synthesis, improve muscle mass production, stimulate post-exercise recovery,
19 enhance immune function, and improve insulin secretion, most likely through the
20 rapamycin (mTOR) signaling pathway (Figure 1A)[2-6]. BCAAs from dietary sources are
21 largely absorbed via the gut intestinal tract, bypassing the liver, and delivered to the
22 peripheral tissues[7-11]. The human pathways for BCAA catabolism involve many
23 highly regulated enzymes, and impaired BCAA catabolism caused by genetic defects in
24 pathway enzymes may result in metabolic diseases such as maple syrup urine disease
25 (MSUD), propionic Acidemia (PA), methylmalonic acidemia (MMA), and isovaleryl
26 acidemia (IVA), among others (Figure 1B)[7, 8, 12-14].

27 Frontline treatment for the aforementioned rare metabolic diseases includes dietary
28 protein restriction[15-18]. Patients consume artificially formulated prescription protein
29 food that has been depleted of one or more BCAAs. However, this treatment option is
30 not without drawbacks. Education, poor availability of the proper food or inconvenience
31 all result in poor compliance with the treatment diet, which is even more challenging in
32 less-developed countries or regions. Therefore, treatments that maintain the ability to
33 consume natural protein foods as part of daily dietary intake are a desired option to
34 improve a patient's quality of life[19-22].

35 Advances in synthetic biology techniques have enabled the engineering of microbes as
36 potential therapies for a number of different diseases. For example, the probiotic strain
37 *E. coli* Nissle 1917 (EcN) has been engineered to express multiple enzymes aimed at
38 the metabolism of phenylalanine as a potential treatment for PKU[23]. Similarly, oral
39 delivery of BCAA-degrading engineered microbes could be used as a therapeutic
40 treatment option for BCAA-related metabolic diseases or disorders. Among the BCAAs,
41 leucine is thought to play the most critical role in disease pathogenesis and therefore is
42 targeted for dietary removal in patients with MSUD, IVA, 3-methylglutaconic aciduria
43 type I and 3-hydroxy-3- methylglutaryl-CoA lyase deficiency[14]. In this article, we
44 describe the genetic engineering of a leucine degradation pathway in the widely used
45 probiotic strain, *E. coli* Nissle 1917. Following demonstration of its activity *in vitro*, we
46 applied high throughput screening techniques to optimize the leucine degradation
47 activity of the strain. We show that pathway optimization translates to increased *in vivo*
48 leucine degradation activity in naïve mouse and non-human primate pharmacokinetic
49 models as measured by tracking blood metabolites and a non-invasive, strain-specific
50 urinary biomarker identified during the course of this study. In this work we present a
51 process for the development of the engineered probiotic EcN with a multi-enzyme
52 pathway and its optimization using high throughput screening for a broad therapeutic
53 application targeting BCAA-related human diseases and disorders.

54 **Results**

55 **Leucine-degradation pathways engineered into *E. coli* Nissle 1917**

56 To engineer EcN for leucine degradation, we designed a three-enzyme pathway to
57 catabolize leucine to isopentanol via ketoisocaproate and isopentanal intermediates.
58 This pathway was composed of leucine dehydrogenase (LeuDH, from *Bacillus cereus*),
59 ketoacid decarboxylase (KivD, from *Lactococcus lactis*), and alcohol dehydrogenase
60 (Adh, from *Saccharomyces cerevisiae*) (Figure 2A). To enhance the transport of leucine
61 into EcN, the gene encoding the *E. coli* BCAA transporter BrnQ was also included in the
62 design[24]. The genes encoding the three catabolic pathway enzymes and the BrnQ
63 transporter were assembled as a multi-cistronic operon in a low copy plasmid which
64 was used to transform a genetically modified EcN strain (SYN469) with the following
65 chromosomal changes: 1) genes encoding a second copy of the endogenous high
66 affinity BCAA transporter LivKHMGF to facilitate additional import of leucine 2) deletion
67 of the leucine biosynthetic gene *ilvC* to prevent BCAA production[25], and 3) deletion of
68 the amino acid export gene, *leuE*, to prevent leucine export[26] (Figure 2B, SYN1980).
69 The same plasmid was also used to transform wild type EcN resulting in strain
70 SYN6034 (Figure 2C).
71 Following construction, leucine consumption by both strains was assessed *in vitro*.
72 SYN1980 was able to consume leucine *in vitro* (Figure 2D), and the rates of leucine
73 consumption between SYN1980 and SYN6034 were not significantly different,
74 indicating that the accessory chromosomal modifications in the SYN1980 chassis did
75 not affect the leucine consumption rate of the heterologous pathway (Figure 2D).
76 However, the BrnQ transporter was required for optimal activity of the heterologous

77 pathway, as elimination of the additional copy of BrnQ resulted in a >55% decrease in
78 the leucine consumption rate (Figure 2D, SYN1992 vs SYN1980). Since the accessory
79 modifications did not improve strain activity, focus was shifted to the three pathway
80 enzymes, LeuDH, KivD, or Adh, to explore the potential to improve the rate of leucine
81 degradation. Analysis of leucine pathway intermediates from SYN1980 demonstrated a
82 time-dependent accumulation of ketoisocaproate, suggesting that the KivD enzyme
83 could be a pathway bottleneck limiting maximal leucine degradation (Figure S1B,
84 SYN1980).

85 **Identification of leucine degrading enzymes with increased activity through high**
86 **throughput enzyme homolog screening and the generation of an improved**
87 **leucine consumption strain**

88 To improve the efficiency of leucine degradation, LeuDH, KivD and Adh were optimized
89 using a high throughput enzyme homolog screening and DNA assembly strategy. For
90 each enzyme, a library of ~1,200 homologs was designed to sample the full enzyme
91 sequence space in public sequence databases (Table 1). To enable the required
92 screening throughput, we developed spectrophotometric enzymatic assays for direct or
93 indirect measurement of LeuDH, KivD, and Adh activities in *E. coli* cell lysates (Figure
94 S2), which are amenable to automation for high throughput screening. A total of 1,175
95 candidate LeuDH enzymes were screened for the ability to deaminate leucine. The
96 initial round of screening identified 110 enzymes with activity on leucine. These 110
97 enzymes were further analyzed in a second screen, and 43 LeuDH enzymes had mean
98 activity higher than the *B. cereus* LeuDH expressed in the prototype strain SYN1980

99 (Figure 3A). The best-performing enzyme, LeuD_H from *Cetobacterium ceti*, exhibited a
100 3.4x greater activity than the *B. cereus* LeuD_H (Table S2).

101 Similarly, to identify a superior ketoisovalerate decarboxylase (KivD), a total of 1,296
102 candidate KivD enzymes were screened for decarboxylase activity on ketoisocaproate.
103 Interestingly, the *L. lactis* KivD enzyme in the SYN1980 pathway did not have
104 measurable activity when screened in the high throughput assay, so KivD activity is
105 reported relative to the non-zero activity of the lysate-only negative control. The initial
106 round of screening identified 55 enzymes with decarboxylase activity. The second round
107 of screening demonstrated that >40 KivD enzymes had at least 6- to 8-fold increase in
108 KivD activity relative to the background lysate activity (Figure 3B, Table S3).

109 For Adh enzyme screening, a library of 1,177 candidates was screened for the ability to
110 reduce isopentanal to isopentanol. Similar to KivD in the decarboxylase assay, the *S.*
111 *cerevisiae* ADH2 enzyme in the SYN1980 prototype strain did not exhibit activity in the
112 Adh assay above the non-zero lysate-only background control. The *Equus caballus* Adh
113 was found to have the desired activity on isopentanal during assay development and
114 was used as a positive control for the Adh screens. We identified 55 Adh enzymes with
115 Adh activity in our first round of screening. The second screening round identified 5 Adh
116 enzymes with at least a 20-fold increase in Adh activity relative to the non-zero
117 background lysate activity, and >10-fold higher than the positive control *E. caballus* Adh
118 (Figure 3C, Table S4).

119 The top hits from each individual enzyme screening were assembled into a library of
120 operons. These Leu catabolic operons were synthesized (*leuD_H-kivD-adh*) and cloned
121 into the same plasmid backbone conferring Leu catabolism in SYN1980, replacing the

122 original catabolic genes upstream of *brnQ* (Figure 2B). Complete pathways encoded
123 four-gene operons (*leuDH-kivD-adh-brnQ*) in which the LeuDH, KivD, and Adh enzymes
124 and their cognate ribosome binding sites (RBSs) were varied while the location and
125 identity of the *brnQ* RBS and coding sequence were held constant (Figure S3). Out of
126 the 462 operons designed, 383 were successfully synthesized as plasmids and 354
127 were successfully transformed into the screening chassis SYN469 (SYN001, $\Delta ilvC$,
128 $\Delta leuE$, *lacZ::Ptet-livKHMGF*). The successful library transformants were screened in a
129 high throughput leucine consumption assay to identify operons conferring greater
130 leucine consumption compared to SYN1980. For plate-to-plate standardization, each
131 plate included control strains which harbored the prototype pathway (SYN1980) or
132 variants lacking LeuDH (SYN1980 $\Delta leuDH$) or BrnQ (SYN1980 $\Delta brnQ$). As shown in
133 Figure 3D, strains were ranked based on leucine consumption, and 108 pathways
134 demonstrated mean leucine consumption equivalent to or higher than the prototype
135 pathway in SYN1980. Enzyme origin and RBS information are listed in Table 2.
136 The 3 strains with the highest leucine consumption rates (SYN5721, SYN5722 and
137 SYN5729, all in SYN469 background) were further characterized. As observed in the
138 pathway library screen, all 3 strains consumed leucine at a faster rate than the
139 prototype strain SYN1980 (Figure S1A). Notably, the 3 strains with optimized pathways
140 had drastically reduced levels of ketoisocaproate in the supernatant when compared to
141 the control strains, indicating that a KivD bottleneck was relieved through the pathway
142 optimization campaign (Figure S1B).

143 To understand the impact of leucine-specific host strain chromosomal modifications on
144 the improved leucine-consuming pathways (the *liv* operon, *ilvC*, and *leuE*), plasmids

145 from the top three strains were used to transform wild type EcN, resulting in strains
146 SYN5941, SYN5942 and SYN5943, and the *in vitro* leucine consumption activity was
147 evaluated for each strain (Figure 4). Similar to the prototype pathway (SYN1980 vs.
148 SYN6034, Figure 4), the accessory gene modifications carried in SYN1980-derivative
149 strains did not enhance activity over the wild type chassis strains. We reasoned that
150 reduced host cell engineering would result in better strain fitness; therefore, we chose to
151 move forward with characterization of a single optimized leucine catabolizing pathway in
152 the wild type EcN background (SYN5941).

153 **Biomarker characterization and detection *in vivo***

154 To enable the assessment of strain activity *in vivo*, biomarkers of leucine consumption
155 activity that could be identified in urine were developed. Glucuronidation reaction
156 catalyzed by UDP-glucuronosyltransferase (UGT) is the major pathway for foreign
157 chemical removal in humans as well as other animals[27, 28]. Therefore, we
158 hypothesized that the end product of the leucine degradation pathway in SYN5941,
159 isopentanol, may be converted by UGT into isopentyl glucuronide (IPG) and excreted in
160 urine (Figure 5A)[27, 29, 30]. To test this hypothesis, isopentanol was orally
161 administered to mice at 100, 250 or 500 mg/kg and urine was collected 4 hours later for
162 detection of IPG. Isopentanol administration resulted in a dose-dependent recovery of
163 IPG, with concentrations reaching $2.06 \pm 0.33 \mu\text{mol}$ at the 500 mg/kg dose (Figure 5B).
164 In naïve mice, a single dose of SYN5941 (5.62×10^{10} CFU) resulted in a significant
165 increase in urinary IPG compared to treatment with vehicle or WT EcN (Figure 5C),
166 demonstrating that the strain degraded leucine *in vivo*.

167 To further investigate the potential of using IPG as a strain-specific biomarker for the
168 evaluation of SYN5941 activity in humans, the baseline urinary IPG levels were
169 analyzed from ten healthy human volunteers. All ten subjects were found to have very
170 low background IPG levels (below the limit of detection $\sim 0.16 \mu\text{g/mL}$) (Figure S4). This
171 suggests that IPG may be useful as a clinical biomarker, as the background signal for
172 IPG would not be expected to confound the assessment of EcN leucine degradation
173 activity in humans.

174 **Activity of engineered EcN in non-human primates**

175 We next examined the activity of leucine-consuming EcN strains in non-human primates
176 (NHPs), as these animals have GI physiology and dietary patterns similar to humans.
177 NHPs received a single dose of vehicle or bacteria concomitantly with 7 g of protein in
178 the form of peptone. Leucine levels in plasma peaked approximately 1h post-peptone
179 administration in vehicle-treated animals (Figure 6A). While SYN1980 did not lower the
180 levels of leucine compared to vehicle treated animals, the optimized strain, SYN5941,
181 displayed a statistically significant decrease in plasma leucine $\text{AUC}_{0-6\text{h}}$ with a
182 concomitant increase in urinary IPG (Figure 6B and C). Taken together, these results
183 not only further validate strain activity *in vivo*, but also demonstrate that the strain
184 optimization strategy translated to measurable improvements in leucine consumption *in*
185 *vivo*.

186 **Discussion**

187 Human metabolic diseases and disorders caused by mutations in BCAA metabolic
188 pathways are typically managed by diet, yet this can be a significant burden for patients,
189 and in some cases, poor dietary management can prove to have life-threatening

190 consequences[20, 31]. Even when carefully followed, dietary restriction can cause
191 significant pressure and create negative psychological issues for patients[19-21].
192 Several drugs are currently in development as treatments for diseases caused by
193 mutations in BCAA metabolic pathways. For example, the small molecule, sodium
194 phenylbutyrate, increases the activity of the branched-chain alpha-keto acid
195 dehydrogenase enzyme complex and improves BCAA degradation[32]. Other groups
196 have developed therapeutic mRNAs encoding missing or damaged pathway enzymes in
197 PA or MMA patients[33, 34]. However, a challenge remains that each of these types of
198 therapies can only target single pathway enzyme within already small patient
199 populations (Figure 1). The high cost and small patient population results in minimal
200 incentive for new drug development and continuously unmet needs for patients.

201 Synthetic biology brings huge potential to provide a clinical benefit to multiple disease
202 indications with a single strain. Specifically, using engineered microbes to consume the
203 BCAAs from the diet could be a promising alternative therapeutic approach for BCAA-
204 related rare diseases since its strategy is simply to remove the BCAA from the food
205 source itself and could apply to a wide range of patients regardless of the underlying
206 genetic mutation.

207 In addition to inborn errors of metabolism, chronically elevated levels of BCAAs are
208 associated with cardiometabolic diseases such as type 2 diabetes (T2D), obesity, and
209 cardiovascular disease (Figure 1A)[5, 35-37]. Current evidence suggests that elevated
210 BCAAs may not only be biomarkers for cardiometabolic diseases but may also play a
211 role in the pathogenesis of these diseases. Further, reduced BCAA intake from daily
212 food may serve to reduce the long-term risk of cardiometabolic diseases[38-40]. BCAA

213 consuming strains could provide a positive effect on overall metabolic fitness or even
214 make intriguing prophylactic treatments for cardiometabolic diseases[41].

215 EcN was selected as the chassis to develop a strain capable of degrading BCAAs in
216 this work. EcN's safety, in its un-engineered form, has been validated by long-term use
217 in humans, and some trials have been done safely in infants[42-44]. In its engineered
218 form, EcN has demonstrated safety, tolerability, and target engagement in human
219 clinical trials for the treatment of inborn errors of metabolism, such as
220 phenylketonuria[23].

221 In this work, we demonstrated leucine consumption by the engineered and optimized
222 probiotic EcN strain in preclinical animal models as proof of concept for the potential
223 treatment of a broad range of disorders and diseases where leucine is a toxic
224 metabolite. The LeuD_H-KivD-Adh pathway was chosen because it does not require ATP
225 for catalysis and this redox-neutral pathway can operate under anaerobic conditions
226 mimicking the gastrointestinal environment. The proof-of-concept strain SYN1980
227 demonstrated that EcN could be engineered to consume leucine *in vitro*, with the
228 leucine importer BrnQ being essential for optimal activity, yet this strain did not
229 significantly lower leucine levels *in vivo*. To improve strain activity, a high throughput
230 campaign targeting key enzymes was conducted and resulted in a ~ 3 x enhancement
231 in the rates of leucine-consumption. Pathway improvements translated to improved
232 leucine degradation rates *in vivo*, as the optimized strain exhibited significant leucine
233 consumption in both mouse and NHP models.

234 Assessing the therapeutic activity of drugs *in vivo* is enabled by the ability to measure
235 biomarker levels on samples collected using non-invasive procedures. Here we

236 identified a non-invasive method to measure isopentanol, the end product of leucine-
237 consuming strains, through identification of IPG, a glucuronic acid conjugate easily
238 measured in urine. The virtually non-existent background levels of IPG in human urine
239 make this a candidate biomarker for further development to provide a strain-specific
240 metabolite to monitor strain activity.

241 This work demonstrates the power of high throughput enzyme homolog screening to
242 identify enzymes and their combinations with increased activity by exploring natural
243 enzyme diversity and to balance metabolic pathways by exploring a large combinatorial
244 design space. Our results here also provide the first example of successful translation of
245 this *in vitro* improvement into *in vivo* biological activity and thus could be considered a
246 valid approach for engineered probiotic strain improvement for therapeutic development
247 in general.

248 **Acknowledgements**

249 Thanks to Dave Hava and Vincent Isabella for suggestions on drafting the manuscript
250 and Yves Millet for the initial design and construction.

251 **Author Contributions**

252 N.L. and C.K. conceived the project. P.B. and A.T. designed the screening studies. N.L.,
253 and J.G. designed and performed bacterial engineering and *in vitro* bacterial analysis.
254 L.R. and M.P. designed the *in vivo* studies and performed the data analysis with L.R.
255 performed the *in vivo* experiment. M.J. and M.J.C. developed mass spectrometry
256 method and detected *in vivo* biomarker. C.B. devised fermentation conditions and
257 provided essential materials. R.J., K.Z. and L.S. designed the high throughput enzyme
258 screening with R.J. and K.Z. conducted the assay. S.M. developed methods and

259 executed metabolites detection assays. S.G. constructed pathway strains. R.P.
260 developed high throughput leucine consumption assay. R.P. and S.G. executed high
261 throughput leucine consumption assay. A.C. sourced and designed enzyme libraries
262 and designed pathway libraries. N.L. and A.T. supervised the project and wrote the
263 manuscript with assistance from C.K..

264 **Data Availability**

265 All engineered strains described in this manuscript can be made available subject to a
266 Material Transfer Agreement (MTA), which can be requested by contacting the
267 corresponding authors. All requests will be reviewed by Synlogic and Ginkgo Bioworks
268 to verify whether the request is subject to any intellectual property or confidentiality
269 obligations. Additional data underlying the figures and supplementary information are
270 available from the corresponding authors on reasonable request.

271 **Figure Legends**

272 **Figure 1. Branched chain amino acids and human diseases. A)** Branched chain
273 amino acids (BCAAs) are essential amino acids which humans must obtain from protein
274 food. They benefit human health but also are believed to relate to various diseases and
275 disorders. **B)** Abnormal degradation of branched chain amino acids due to defective
276 enzymes in human will result in severe disorders such as maple syrup urine disease
277 (MSUD), propionic acidemia (PA), methylmalonic acidemia (MMA), isovaleryl acidemia
278 (IVA), or 3-methylcrotonyl-CoA carboxylase deficiency (3-MCC).

279 **Figure 2. BCAA degradation pathway design, strain construction and *in vitro***
280 **activity. A)** Leucine consumption pathway designed to engineer into EcN in this study.

281 **B)** The scheme of prototype strain SYN1980. **C)** The scheme of prototype strain
282 SYN6034. **D)** *In vitro* leucine consumption of engineered prototype strains (n = 2 for
283 each timepoint and the error bar indicates the range of duplicates, solid lines indicate
284 the linear regression fit of means for each strain).

285 **Figure 3. High throughput enzyme and operon screening results.** **A)** The top 110
286 LeuDH enzymes from the primary screen were re-screened to validate enzyme activity
287 (n = 4). Activities are reported as fold-improvement over the *B. cereus* LeuDH activity
288 (green dot and green dashed line). **B)** The top 55 KivD enzymes from the primary
289 screen were re-screened for activity (n = 4). Activities are reported as fold-improvement
290 over of *L. lactis* KivD, which was equivalent to the non-zero assay background (green
291 dashed line). **C)** Top 55 Adh enzymes from the primary screen were re-screened for
292 activity (n = 4). Since the strain expressing *S. cerevisiae* ADH2 had no measurable
293 activity in this assay, activities are reported relative to *E. caballus* Adh (green dot, green
294 dashed line). **D)** Pathway operons with optimized enzymes were screened for leucine
295 consumption. Strains were assayed in biological replicates (n = 2 or 3, depending on the
296 number of successful transformants). Data points are shown as dots, and the average
297 for each strain is shown as a horizontal blue line. Control and reference strains are
298 indicated with colored labels.

299 **Figure 4. Confirmation of leucine consumption activity of the top strains after**
300 **scaling up in fermenter.** Original host strain was used as the chassis to test the
301 activity (SYN1980, SYN5721, SYN5722, SYN5729, solid symbols with solid lines
302 indicating the linear regression fit of means). The same four plasmids were also
303 transformed into wild type EcN strain resulting in strains SYN6034, SYN5941,

304 SYN5942, SYN5943). The corresponding *in vitro* activity was measured (empty symbols
305 with dotted line indicating the linear regression fit of means).

306 **Figure 5. *In vivo* biomarker validation and strain activity in mice. A)** Proposed
307 pathway of *in vivo* isopentyl glucuronide (IPG) formation. **B)** IPG urinary recovery in
308 response to oral administration of isopentanol in mice (n = 5 for each group). Statistical
309 analysis was performed using one-way ANOVA followed by Tukey's multiple
310 comparison test (**** $p < 0.0001$, *** $p < 0.0007$ versus vehicle). **C)** IPG urinary recovery
311 in response to orally administered leucine consuming strain SYN5941 in mice (n = 5 for
312 each group, bacterial dosed at 0 h, 1 h and 2 h and totaled at 5.62×10^{10} cells). All vehicle
313 & SYN094 samples are below limit of quantification = $0.00003 \mu\text{mol}$. Statistical analysis
314 was performed using two-way ANOVA analysis followed by Tukey's multiple
315 comparison test (**** $p < 0.0001$ versus vehicle).

316 **Figure 6. Efficacy of SYN1980 or SYN5941 in healthy nonhuman primates. A)**
317 Effect of SYN1980 and SYN5941 on plasma leucine levels following oral administration
318 of leucine consuming strains. Statistical analysis was performed using two-way ANOVA
319 analysis followed by Tukey's multiple comparison test (* $p < 0.05$ versus vehicle). **B)**
320 Quantification of area under the curves (AUC) from plot A in this figure. Statistical
321 analysis was performed using ordinary one-way ANOVA analysis (** $p < 0.0051$ versus
322 vehicle) followed by Tukey's multiple comparison test. **C)** Urinary IPG recovery following
323 oral administration of leucine consuming strains. Statistical analysis was performed
324 using one-way ANOVA analysis followed by Tukey's multiple comparison test (** $p <$
325 0.005 versus vehicle).

Material and Methods

Strain construction

Refer below to Table S1 for a list of strains used in this publication. *Escherichia coli* Nissle 1917 (EcN), designated as SYN001 here, was purchased from the German Collection of Microorganisms and Cell Cultures (DSMZ Braunschweig, *E. coli* DSM 6601).

The deletion of the *ilvC* and *leuE* gene was conducted by using P1 transduction from the corresponding BW25113 strains and the removal of antibiotic resistance cassettes via pCP20 and subsequent pCP20 removal. Insertion of *Ptet-ilvKHPMF* cassette at *lacZ* locus was carried out by the lambda red recombineering method via pKD46 and subsequent pKD46 removal, followed by the removal of antibiotic resistance cassettes via pCP20 and subsequent pCP20 removal. For constructing plasmids, DNA fragments containing the BCAA-consuming operon under the control of various promoters were synthesized at GENEWIZ, IDT DNA, Ginkgo, or PCR-amplified from corresponding vectors from the Synlogic collection and cloned into a Synlogic vector containing an ampicillin resistance gene, a low copy number origin of replication (pSC101) and the regulatory control of the *Ptet* promoter by Gibson assembly method. These plasmids were electroporated into SYN001 or other host strains. After electroporation (Eporator, Eppendorf, 1.8-kV pulse, 1-mm gap length electro-cuvettes), the transformed cells were selected as colonies on LB agar (Sigma, L2897) containing proper antibiotics.

Preparation of strains in flask

For analysis of leucine or other BCAA metabolism, cells were inoculated in 4 mL of 2xYT containing appropriate antibiotics in a 14-mL round bottom tube and incubated at

37 °C with shaking at 250 RPM overnight. The next day, cell cultures were diluted 1:100 in 50 mL of FM1 medium in 125-mL baffled flasks at 37 °C with shaking (250 RPM) for 2h, also with appropriate antibiotics. Cells were induced with the addition of anhydrous tetracycline (Sigma, ATC, 100 ng/mL final concentration) or IPTG (Sigma, 1 mM final concentration). All induction proceeded for 4h. Following induction, cells were centrifuged for 5 minutes at 8000 x g at 4 °C, washed once with an ice-cold formulation buffer (KH₂PO₄ (2.28 g/L) and K₂HPO₄ (14.5 g/L)) containing 15% of glycerol (pH 7.5). Finally, cells were concentrated 20-fold in the formulation buffer and stored at 80°C until the days of testing.

Preparation of strains in fermenter

A seed flask fermentation was started from a scraping of the frozen MCB culture in a cryovial with an inoculum loop into a 500-mL baffled flask with 50 mL FM1 media supplemented with 25 g/L glucose or FM2 media supplemented with 40 g/L glycerol and 100 µg/mL carbenicillin. This culture was grown overnight for ~15-16h at 37 °C and shaken at 350 RPM. Next day, a seed culture of ~30-40 OD₆₀₀ was used to inoculate a fermentation vessel with corresponding media and 100 µg/mL carbenicillin to a starting OD₆₀₀ of 0.15. The fermentation was grown at 37 °C and pH 7 with a dissolved oxygen setpoint of 60% for ~6h to achieve final biomass production. The fermentation growth phase was allowed to multiply for 2h until the OD₆₀₀ reached 1.5-3. At the target OD, the culture was induced by ATC at a final concentration of 600 ng/mL to activate the cells. The induction of cells continued for 4h until the generation of final biomass reached between 20-30 OD₆₀₀. Fermentation was harvested at 4h post-induction endpoint and

spun down by centrifuging culture broth for 30 min at ~ 5000 g at 4 °C. Cells were finally resuspended in glycerol/phosphate buffer, aliquoted and stored at -80°C.

***In vitro* strain activity assays**

Frozen cells were thawed on ice and washed once with ice-cold MMG medium (M9 medium (Becton Dickinson) supplemented with 50 mM MOPS (3-(N-morpholino)propanesulfonic acid) and 0.5% glucose). Cell concentration was determined by measuring OD₆₀₀ with a spectrophotometer (1 OD₆₀₀ = 1e⁹ cells/mL). Washed cells were diluted to 2e⁹ cells/mL in MMG medium and 800 µL of the cell suspension was transferred into a well of a 96-deepwell plate, followed by addition and mixing of equal volume of assay media (MMG containing 20 mM leucine) using a multichannel pipet. The plate was covered by a breathe-EASIER membrane (Diversified Biotech, MA) and incubated statically at 37 °C in an anaerobic chamber. Bacterial broth samples were taken at specified time and centrifuged immediately for 10 minutes at 2270 x g and 4 °C. Supernatants were transferred into wells of a new plate and used for HPLC or LC-MS analysis.

Enzyme library design and construction

For each enzyme, a library of ~1,200 homologs was designed to sparsely sample all sequences in public sequence databases. Machine-learning-based bioinformatics tools were used to identify enzyme candidates for each of the three desired activities (leucine dehydrogenase, 1.4.1.9; ketoisovalerate decarboxylase, 4.1.1.1; and alcohol dehydrogenase 1.1.1.1) in public sequence databases (SwissProt and TrEMBL, together known as UniProt). DNA sequences encoding all library enzymes were optimized for expression in *E. coli*, synthesized in an inducible *E. coli* expression vector

under the control of the T7 promoter and transformed into *E. coli* for high throughput screening.

Cultivation conditions for enzyme assays

For each of the enzyme libraries screened, strains harboring library plasmids were transformed into *E. coli* T7 expression host cells. 5 μ L of thawed glycerol stocks were stamped into 500 μ L/well of LB + 100 μ g/mL carbenicillin (LB-Carb100) in half-height deepwell plates, which were sealed with AeraSeals. Samples were incubated at 37 °C and shaken at 1000 RPM in 80% humidity overnight. 50 μ L/well of the resulting precultures were stamped into 450 μ L/well of LB-Carb100 + 1 mM IPTG in half-height deepwell plates, which were sealed with AeraSeals. Samples were incubated at 30°C and shaken at 1000 RPM in 80% humidity overnight. 250 μ L/well of the resulting production cultures were stamped into deepwell plates containing 500 μ L of phosphate buffered saline (PBS) and centrifuged for 10 minutes at 4000 x g. Supernatant was removed and the resulting cell pellet was resuspended in 200 μ L of BugBuster Protein Extraction Reagent + 1 μ L/mL purified benzonase + 1 μ L/6 mL purified Lysozyme. Samples were incubated for 10 minutes at room temperature to generate the cell lysates used in *in vitro* enzyme assays.

LeuD_H activity assay

10 μ L of lysate for the LeuD_H library strains was transferred to a half-area flat-bottom plate containing 90 μ L/well assay buffer (20 mM leucine, 200 mM Glycine, 200 mM KCl, 0.4 mM NAD, pH 10.5). Optical measurements were taken on a plate reader, with absorbance readings taken at 340 nm for 10 minutes. The resulting kinetic data was used to resolve the maximum rate of NAD⁺ reduction, a proxy for LeuD_H activity.

KivD activity assay

10 μ L of lysate for the KivD library strains was transferred to a half-area flat-bottom plate containing 90 μ L/well assay buffer (100 mM PIPES-KOH, 100 mM potassium glutamate, 1 mM dithiothreitol, 0.4 mM NAD, 1.5 mM thiamine pyrophosphate, 10 mM magnesium glutamate, 20 mM ketoisocaproate (KIC), 1 U/mL *S. cerevisiae* aldehyde dehydrogenase pH 7.5). The coupling enzyme (*S. cerevisiae* aldehyde dehydrogenase) was used to indirectly measure KivD activity on KIC. Optical absorbance measurements were taken over 10 minutes. The resulting kinetic data was used to determine KivD activity.

Adh activity assay

10 μ L of lysate for the Adh library strains was transferred to a half-area flat-bottom plate containing 90 μ L/well assay buffer (50 mM MOPS buffer, 0.4 mM NADH, and 30 mM isovaleraldehyde, pH 7.0). Optical absorbance measurements were taken on a plate reader at 340 nm for 10 minutes. The resulting kinetic data was used to resolve the maximum rate of NADH oxidation, a proxy for ADH activity.

Pathway enzyme selection and operon library assembly

Selected top enzymes were incorporated in the final operon designs with various RBS strength to balance flux of the leucine-consuming pathway. Among the 3 RBSs, two were designed using the RBS Calculator to have translation initiation rates of approximately 5,000 au and approximately 50,000 au[45-48]. In addition to designing two conventional RBSs for each enzyme, we also included an RBS that was co-translationally coupled to a short leader peptide, in what is termed a bicistronic design[49]. RBS-enzyme pairs were assembled into a partial combinatorial library of

462 pathways. Each pathway contains either conventional RBSs or BCD-type RBSs, but not both. The gene order was held constant (*leuDH-kivD-adh*).

These leucine catabolic pathways were synthesized (*leuDH-kivD-adh*) and cloned into the same plasmid backbone conferring leucine catabolism in SYN1980, replacing the original catabolic genes upstream of *brnQ*. Complete pathways encoded four-gene operons (*leuDH-kivD-adh-brnQ*) in which the LeuDH, KivD, and Adh enzymes and their cognate RBSs are varied while the location and identity of the *brnQ* RBS and coding sequence are held constant. Out of the 462 operons designed, 383 were successfully synthesized as plasmids and 354 were successfully transformed into the screening chassis SYN469 (SYN001, $\Delta ilvC$, $\Delta leuE$, *lacZ::Ptet-livKHMGF*).

Operon screening

The successful library transformants were screened in a high throughput leucine consumption assay to identify operons conferring greater leucine consumption compared to SYN1980. All pathway-containing strains were cultured and screened for leucine consumption in 96-well plates. For plate-to-plate standardization, each plate included control strains which harbored the prototype pathway (SYN1980) or variants lacking LeuDH (SYN1980 $\Delta leuDH$) or BrnQ (SYN1980 $\Delta brnQ$).

Ethical statement

All procedures performed on animals were in accordance with the humane guidelines for ethical and sensitive care by the Institutional Animal Care and Use Committee (IACUC) of the U.S. National Institutes of Health. Procedures and protocols related to mouse studies were reviewed and approved by Mispro Biotech Services' Institutional Animal Care and Use Committee. Standard operating procedures related to NHP

studies have been reviewed and approved by Charles River Laboratories' Institutional Animal Care and Use Committee.

Biomarker study in mice

A total of 72 female C57BL/6J mice aged 19 weeks, from Jackson Laboratories, were acclimated for a minimum of 4 days. The vehicle control used for this study was filtered water, and the Isopentanol chemical compound was pharmaceutical grade 3-methyl-1-butanol (Sigma Aldrich). Mice were tail marked with a Sharpie marker, weighed, and randomized by body weight into 4 groups each containing 18 mice. Group 1 animals were given a 200 μ L oral gavage dose of water, Group 2 animals were given a 200 μ L oral gavage dose of 100 mg/kg isopentanol, Group 3 animals were given a 200 μ L oral gavage dose of 250 mg/kg isopentanol, and Group 4 animals were given a 200 μ L oral gavage dose of 500 mg/kg isopentanol. Once dosing was completed the animals were placed 3 per cage into metabolic cages (Tecniplast 3600M021) with *ad libitum* access to food and water. After a period of 4 hours the animals were individually removed from the metabolic cages and urine was collected by free-catch into an Eppendorf tube. The free-catch urine was then combined with the urine collected from the metabolic cage and samples were plated for analysis.

Non-human primate (NHP) study

A total of twelve male cynomolgus non-human primates (NHP), approximately 2-5 years of age, were housed at the Charles River Laboratories (CRL) where studies were conducted by experienced staff members. Samples were collected at CRL and shipped to Synlogic where they were plated for analysis. Due to the limited number of animals available per study, three separate studies were conducted, and the results were

combined for analysis. In each study NHP's were separated into two groups. Each group was orally dosed into the stomach with three compounds; 14 mL of peptone (500 g/L), followed by 7.8 mL of vehicle (PBS + 15% glycerol) or bacteria (SYN1980 or SYN5941), followed by 5 mL of 0.36 M bicarbonate, and then finally a small amount of water to rinse the material from the gavage tube. The animals were then placed individually into cages with clean urine collection pans. After a period of 6 hours the urine pans were removed, and the urine was collected into 50-mL tubes and weighed. Study 1 (NHP20192881) had 12 NHP's separated into 6 animals for group 1 receiving SYN1980 bacteria, and 6 animals for group 2 receiving SYN5941 bacteria. Study 2 (NHP20192884) had 11 NHP's separated into 5 animals for group 1 receiving Vehicle, and 6 animals for group 2 receiving SYN5941 bacteria. Study 3 (NHP20197305) had 11 NHP's separated into 5 animals for group 1 receiving Vehicle, and 6 animals for group 2 receiving SYN1980 bacteria.

Statistical analysis

Raw data generated was entered in a Microsoft Excel (Microsoft, Seattle, WA) spreadsheet and transferred to GraphPad Prism 8.0 (GraphPad Software, San Diego, CA). Statistical analysis was performed using GraphPad Prism and the statistical analysis was performed using two-way ANOVA followed by Tukey's multiple comparison test. Significance was set as $p < 0.05$.

HPLC analysis

A Shimadzu Prominence-i LC-2030C HPLC system was used. For leucine analysis, the analytical column was Luna 5 mm C18(2) LC column (50 x 2 mm) (Phenomenex) fitted with a guard column (4 x 2 mm) of the same type. The mobile phase was composed

potassium phosphate buffer (0.02 M; pH 6.9) (A) and acetonitrile–methanol–water (45:40:15, v/v/v) (B) under isocratic elution condition: 70% A and 30% B for 5 min at a flow rate 0.5 mL/min. For analysis of leucine, the analytical column was Luna 5 μm C18(2) LC column (100 x 2 mm) (Phenomenex) fitted with the same guard column and isocratic elution condition was the same except for running for 10 minutes. The supernatants were derivatized with OPA reagent (Agilent) according to the manufacturer's instruction and 3 μL of derivatized samples was injected into the column. The absorbance detector was set at 338 nm and the temperature of the column was maintained at 40 °C. Leucine quantitated in bacterial supernatant, plasma, and urine by liquid chromatography coupled to tandem mass spectrometry (LC-MS/MS) using either an Ultimate 3000 UHPLC-TSQ Quantum or a Vanquish UHPLC-TSQ Altis system. Samples were extracted with 9 parts 2:1 acetonitrile:water containing 1 μg/mL leucine-d₃ as an internal standard, vortexed, and centrifuged. Supernatants were diluted with 9 parts 0.1% formic acid and analyzed concurrently with standards processed as above from 0.8 to 1000 μg/mL. Samples were separated on a Phenomenex Synergi 4 μm Hydro-RP 80A, 75 x 2 mm using a 0.1% formic acid (A), 0.1% formic acid/acetonitrile (B) at 0.3 mL/min and 50 °C. After a 2 μL injection and an initial 5% B hold from 0 to 0.5 minutes, analytes were gradient eluted from 5 to 90% B over 0.5 to 1.5 minutes followed by high organic wash and aqueous equilibration steps. Analytes were detected using Selected Reaction Monitoring (SRM) of compound specific collision induced fragments in electrospray positive ion mode (leucine: 132>86). SRM chromatograms were integrated and the unknown/internal standard peak area ratios were used to calculate concentrations against the standard curve.

GC-MS quantitation of isopentanol

Quantitation of isopentanol in bacterial supernatant and urine samples was performed using Agilent gas chromatography-mass spectrometry (GC-MS) with Restek Stabilwax-MS 30 m x 0.25 mm x 0.25 μ m column. Briefly, 500 μ L of extraction solution was added to 100 μ L of samples. Extraction solution was prepared by spiking 10 μ L Isopentanol-d11 (10 mg/mL) in 5 mL ethyl acetate for a final concentration of 20 μ g/mL isopentanol-d11. The samples were then mixed vigorously and centrifuged at 16,000 x g for 15 mins at room temperature. The following are the GC-MS parameters used for the analysis: 1 μ L injection volume; gas (He) flow rate of 1 mL/min; 40 °C for 5 minutes, ramped to 220 °C for 3.6 minutes, and held at 220 °C for 5 minutes. Selected ion monitoring (SIM) was used for quantitative MS analysis. The following target ions were monitored for quantitation: isopentanol (55.1) and internal standard isopentanol-d11 (62.2).

LC-MS/MS quantitation of isopentyl glucuronide

Isopentyl glucuronide was quantified using a liquid chromatography triple quadrupole tandem mass spectrometry (LC-MS/MS) Thermo TSQ Altis system. In a conical bottom plate, 10 μ L of standards and samples were diluted with 90 μ L water containing 5 μ g/mL of internal standard (Isopentyl-glucuronide-d11).

Chromatographic gradient separation was carried out using an Accucore aQ C18 column 2.6 μ m 100 Å, 100 x 2.1 mm column at 40 °C with mobile phases 10 mM ammonium acetate in water (A) and 10 mM ammonium acetate in acetonitrile (B).

Multiple reaction monitoring in negative mode was used for tandem MS analysis. The following mass transitions were monitored for quantitation: isopentyl glucuronide (263.1/75) and internal standard isopentyl glucuronide-d11 (274.1/75).

LC-MS/MS method for leucine quantification

Leucine was quantified in bacterial supernatant by liquid chromatography coupled to tandem mass spectrometry (LC-MS/MS) using either an Ultimate 3000 UHPLC-TSQ Quantum or a Vanquish UHPLC-TSQ Altis system. Samples were extracted with 9 parts of acetonitrile : water = 2 :1 containing 1 µg/mL leucine-d3 as an internal standard, vortexed, and centrifuged. Supernatants were diluted with 9 parts 0.1% formic acid and analyzed concurrently with standards processed as above from 0.8 to 1000 µg/mL. Samples were separated on a Phenomenex Synergi 4 µm Hydro-RP 80A, 75 x 2 mm using a 0.1% formic acid (A), 0.1% formic acid/acetonitrile (B) at 0.3 mL/min and 50°C. After a 2 µL injection and an initial 5% B hold from 0 to 0.5 minutes, analytes were gradient eluted from 5 to 90% B over 0.5 to 1.5 minutes followed by high organic wash and aqueous equilibration steps. Analytes were detected using Selected Reaction Monitoring (SRM) of compound specific collision induced fragments in electrospray positive ion mode (leucine: 132>86, isoleucine: leucine-d3: 135>89). SRM chromatograms were integrated, and the unknown/internal standard peak area ratios were used to calculate concentrations against the standard curve.

LC-MS methods for pathway intermediates

Leucine (Leu), ketoisocaproate (KIC), and isovaleraldehyde (IVA) were detected by LCMS analysis performed on a Thermo Ultimate 3000 UPLC system with a Thermo Q-Exactive quadrupole-orbitrap mass detector and a Thermo Accucore PFP column (2.1 x 100 mm, 2.6 µm packing) using the following elution solvents: A=0.1% formic acid and 0.1% TFA in water; B=0.1% formic acid in acetonitrile. The gradient was at 0.5 mL/min of 1% B in A for 60 seconds, followed by a linear ramp from 1% to 40% B over 270

seconds. The column is then flushed with 95% B in A for 60 seconds, and re-equilibrated with 1% B in A for 180 seconds. MS acquisition was from 0.8 to 5.3 minutes. Column effluent is introduced into the mass spectrometer via a standard Thermo ESI source with positive mode ionization at +3800V, vaporizer temperature of 400 °C, and ion transfer tube temperature of 375 °C. Thermo reports gas flow rates in arbitrary units probably approximating L/min at STP. Set points were: sheath gas, 60; aux gas, 30; sweep gas, 1. To increase data acquisition rate, orbitrap resolution was set to 17,500. Quadrupole resolution was 1 m/z. 2-(Dimethylamino)ethylhydrazine was used to derivatize both aldehydes and keto acids for analysis in positive mode. A buffer of 0.5 M acetic acid and 0.5 M sodium acetate in methanol was used for the quantification of leucine acid and leucine aldehyde, while also measuring non-derivatized leucine.

References

1. Holeček, M., *Branched-chain amino acids in health and disease: metabolism, alterations in blood plasma, and as supplements*. Nutrition & Metabolism, 2018. **15**(1): p. 33.
2. Neishabouri, S.H., S.M. Hutson, and J. Davoodi, *Chronic activation of mTOR complex 1 by branched chain amino acids and organ hypertrophy*. Amino Acids, 2015. **47**(6): p. 1167-1182.
3. Nair, K.S. and K.R. Short, *Hormonal and Signaling Role of Branched-Chain Amino Acids*. The Journal of Nutrition, 2005. **135**(6): p. 1547S-1552S.
4. Jewell, J.L., R.C. Russell, and K.-L. Guan, *Amino acid signalling upstream of mTOR*. Nature Reviews Molecular Cell Biology, 2013. **14**(3): p. 133-139.
5. Lynch, C.J. and S.H. Adams, *Branched-chain amino acids in metabolic signalling and insulin resistance*. Nature Reviews Endocrinology, 2014. **10**(12): p. 723-736.
6. Gingras, A.C., B. Raught, and N. Sonenberg, *Regulation of translation initiation by FRAP/mTOR*. Genes Dev, 2001. **15**(7): p. 807-26.
7. Brosnan, J.T. and M.E. Brosnan, *Branched-chain amino acids: enzyme and substrate regulation*. J Nutr, 2006. **136**(1 Suppl): p. 207S-115.
8. Harper, A.E., R.H. Miller, and K.P. Block, *Branched-chain amino acid metabolism*. Annu Rev Nutr, 1984. **4**: p. 409-54.
9. Hutson, S.M., *Regulation of substrate availability for the branched-chain alpha-keto acid dehydrogenase enzyme complex*. Ann N Y Acad Sci, 1989. **573**: p. 230-9.
10. Hutson, S.M. and T.R. Hall, *Identification of the mitochondrial branched chain aminotransferase as a branched chain alpha-keto acid transport protein*. J Biol Chem, 1993. **268**(5): p. 3084-91.

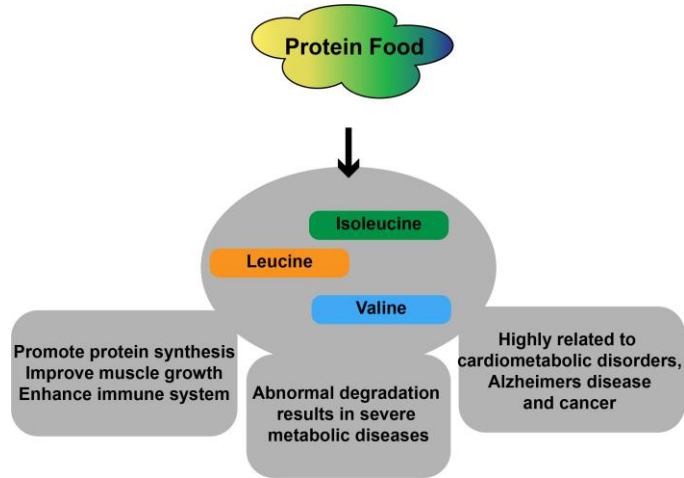
11. Adeva-Andany, M.M., et al., *Enzymes involved in branched-chain amino acid metabolism in humans*. *Amino Acids*, 2017. **49**(6): p. 1005-1028.
12. Fraser, J.L. and C.P. Venditti, *Methylmalonic and propionic acidemias: clinical management update*. *Curr Opin Pediatr*, 2016. **28**(6): p. 682-693.
13. Tanaka, K., et al., *Isovaleric acidemia: a new genetic defect of leucine metabolism*. *Proc Natl Acad Sci U S A*, 1966. **56**(1): p. 236-42.
14. Manoli, I. and C.P. Venditti, *Disorders of branched chain amino acid metabolism*. *Transl Sci Rare Dis*, 2016. **1**(2): p. 91-110.
15. Hauser, N.S., et al., *Variable dietary management of methylmalonic acidemia: metabolic and energetic correlations*. *Am J Clin Nutr*, 2011. **93**(1): p. 47-56.
16. Frazier, D.M., et al., *Nutrition management guideline for maple syrup urine disease: an evidence- and consensus-based approach*. *Mol Genet Metab*, 2014. **112**(3): p. 210-7.
17. Lea, D., et al., *Dietary Management of Propionic Acidemia: Parent Caregiver Perspectives and Practices*. *JPEN J Parenter Enteral Nutr*, 2019. **43**(3): p. 434-437.
18. Pinto, A., et al., *Dietary practices in isovaleric acidemia: A European survey*. *Mol Genet Metab Rep*, 2017. **12**: p. 16-22.
19. Packman, W., et al., *Psychosocial issues in families affected by maple syrup urine disease*. *J Genet Couns*, 2007. **16**(6): p. 799-809.
20. De Castro-Hamoy, L.G., et al., *Challenges in the management of patients with maple syrup urine disease diagnosed by newborn screening in a developing country*. *J Community Genet*, 2017. **8**(1): p. 9-15.
21. Packman, W., et al., *Young adults with MSUD and their transition to adulthood: psychosocial issues*. *J Genet Couns*, 2012. **21**(5): p. 692-703.
22. Simon, E., M. Schwarz, and U. Wendel, *Social outcome in adults with maple syrup urine disease (MSUD)*. *J Inher Metab Dis*, 2007. **30**(2): p. 264.
23. Isabella, V.M., et al., *Development of a synthetic live bacterial therapeutic for the human metabolic disease phenylketonuria*. *Nat Biotechnol*, 2018. **36**(9): p. 857-864.
24. Zhu, J., et al., *Enhancement of precursor amino acid supplies for improving bacitracin production by activation of branched chain amino acid transporter BrnQ and deletion of its regulator gene *lrp* in *Bacillus licheniformis**. *Synth Syst Biotechnol*, 2018. **3**(4): p. 236-243.
25. Li, K.H., et al., *Biological Functions of *ilvC* in Branched-Chain Fatty Acid Synthesis and Diffusible Signal Factor Family Production in *Xanthomonas campestris**. *Front Microbiol*, 2017. **8**: p. 2486.
26. Kutukova, E.A., et al., *The *yeaS* (*leuE*) gene of *Escherichia coli* encodes an exporter of leucine, and the *Lrp* protein regulates its expression*. *FEBS Lett*, 2005. **579**(21): p. 4629-34.
27. King, C.D., et al., *UDP-glucuronosyltransferases*. *Curr Drug Metab*, 2000. **1**(2): p. 143-61.
28. Ritter, J.K., *Roles of glucuronidation and UDP-glucuronosyltransferases in xenobiotic bioactivation reactions*. *Chem Biol Interact*, 2000. **129**(1-2): p. 171-93.
29. Kamil, I.A., J.N. Smith, and R.T. Williams, *The metabolism of aliphatic alcohols; glucuronide formation*. *Biochem J*, 1951. **49**(3): p. xxxviii.
30. Webley, D.M. and P.C. De Kock, *The metabolism of some saturated aliphatic hydrocarbons, alcohols and fatty acids by *Proactinomyces opacus* Jensen (*Nocardia opaca* Waksman & Hendrik)*. *Biochem J*, 1952. **51**(3): p. 371-5.
31. MacDonald, A., et al., *Adherence issues in inherited metabolic disorders treated by low natural protein diets*. *Ann Nutr Metab*, 2012. **61**(4): p. 289-95.
32. Zubarioglu, T., et al., *Impact of sodium phenylbutyrate treatment in acute management of maple syrup urine disease attacks: a single-center experience*. *J Pediatr Endocrinol Metab*, 2020.
33. An, D., et al., *Systemic Messenger RNA Therapy as a Treatment for Methylmalonic Acidemia*. *Cell Rep*, 2017. **21**(12): p. 3548-3558.

34. Jiang, L., et al., *Dual mRNA therapy restores metabolic function in long-term studies in mice with propionic acidemia*. Nat Commun, 2020. **11**(1): p. 5339.
35. Wang, T.J., et al., *Metabolite profiles and the risk of developing diabetes*. Nat Med, 2011. **17**(4): p. 448-53.
36. Asghari, G., et al., *High dietary intake of branched-chain amino acids is associated with an increased risk of insulin resistance in adults*. J Diabetes, 2018. **10**(5): p. 357-364.
37. Zheng, Y., et al., *Cumulative consumption of branched-chain amino acids and incidence of type 2 diabetes*. Int J Epidemiol, 2016. **45**(5): p. 1482-1492.
38. Fontana, L., et al., *Decreased Consumption of Branched-Chain Amino Acids Improves Metabolic Health*. Cell Rep, 2016. **16**(2): p. 520-530.
39. Cummings, N.E., et al., *Restoration of metabolic health by decreased consumption of branched-chain amino acids*. J Physiol, 2018. **596**(4): p. 623-645.
40. Karusheva, Y., et al., *Short-term dietary reduction of branched-chain amino acids reduces meal-induced insulin secretion and modifies microbiome composition in type 2 diabetes: a randomized controlled crossover trial*. Am J Clin Nutr, 2019. **110**(5): p. 1098-1107.
41. White, P.J. and C.B. Newgard, *Branched-chain amino acids in disease*. Science, 2019. **363**(6427): p. 582-583.
42. Behnsen, J., et al., *Probiotics: properties, examples, and specific applications*. Cold Spring Harb Perspect Med, 2013. **3**(3): p. a010074.
43. Lodinova-Zadnikova, R. and U. Sonnenborn, *Effect of preventive administration of a nonpathogenic Escherichia coli strain on the colonization of the intestine with microbial pathogens in newborn infants*. Biol Neonate, 1997. **71**(4): p. 224-32.
44. Henker, J., et al., *Probiotic Escherichia coli Nissle 1917 versus placebo for treating diarrhea of greater than 4 days duration in infants and toddlers*. Pediatr Infect Dis J, 2008. **27**(6): p. 494-9.
45. Salis, H.M., E.A. Mirsky, and C.A. Voigt, *Automated design of synthetic ribosome binding sites to control protein expression*. Nat Biotechnol, 2009. **27**(10): p. 946-50.
46. Espah Borujeni, A., A.S. Channarasappa, and H.M. Salis, *Translation rate is controlled by coupled trade-offs between site accessibility, selective RNA unfolding and sliding at upstream standby sites*. Nucleic Acids Res, 2014. **42**(4): p. 2646-59.
47. Espah Borujeni, A. and H.M. Salis, *Translation Initiation is Controlled by RNA Folding Kinetics via a Ribosome Drafting Mechanism*. J Am Chem Soc, 2016. **138**(22): p. 7016-23.
48. Espah Borujeni, A., et al., *Precise quantification of translation inhibition by mRNA structures that overlap with the ribosomal footprint in N-terminal coding sequences*. Nucleic Acids Res, 2017. **45**(9): p. 5437-5448.
49. Mutalik, V.K., et al., *Precise and reliable gene expression via standard transcription and translation initiation elements*. Nat Methods, 2013. **10**(4): p. 354-60.

FIGURES

Figure 1.

A



B

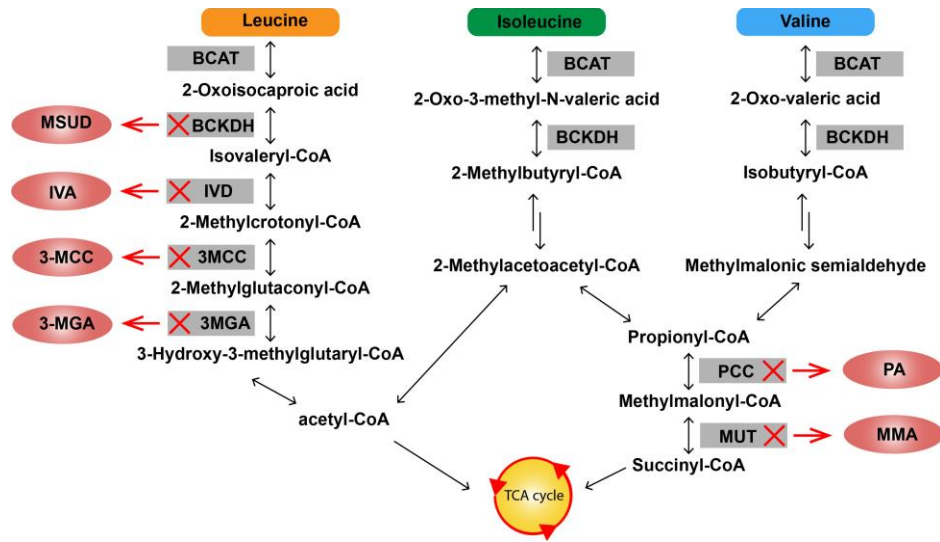
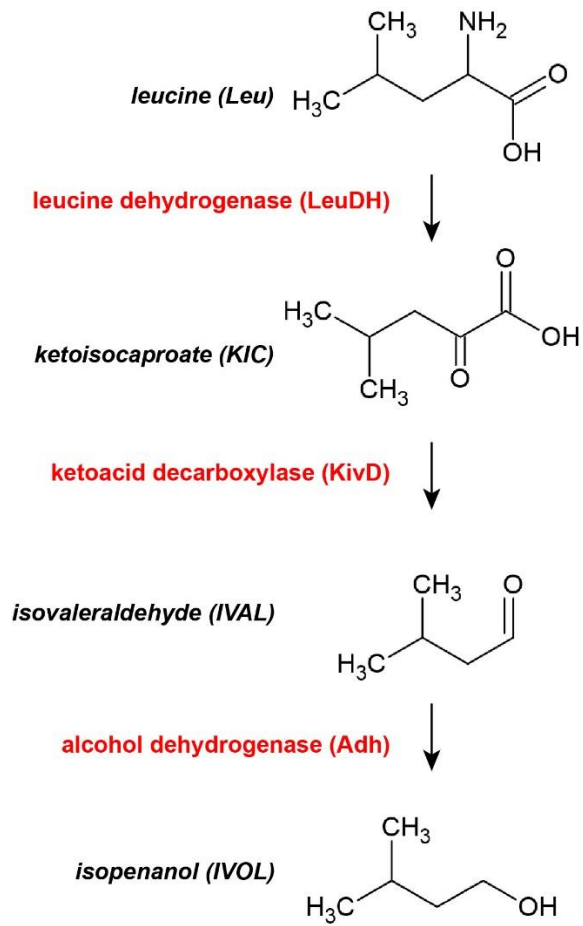
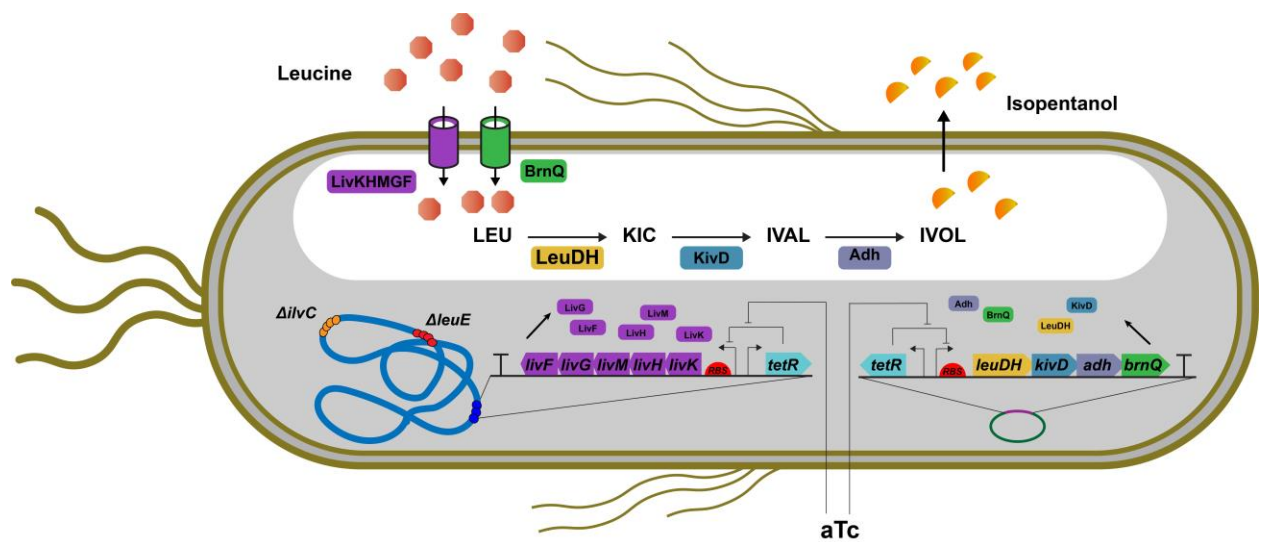


Figure 2.

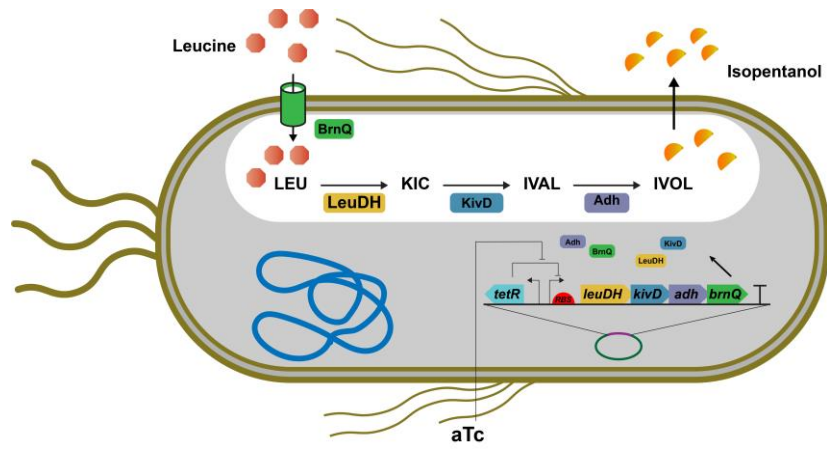
A



B



C



D

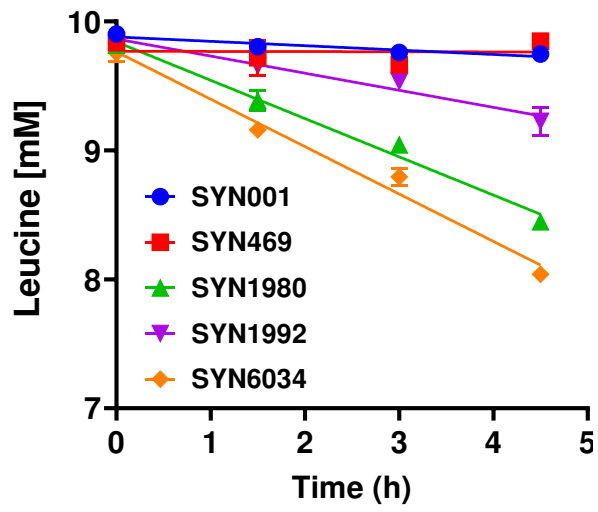


Figure 3.

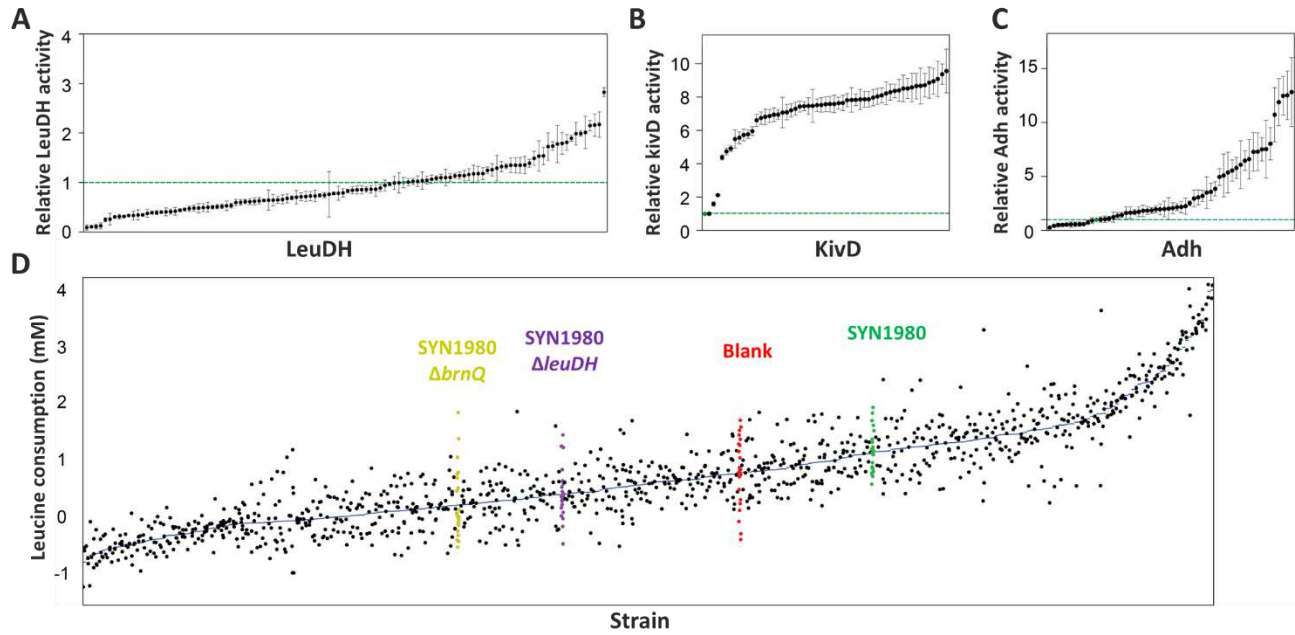


Figure 4.

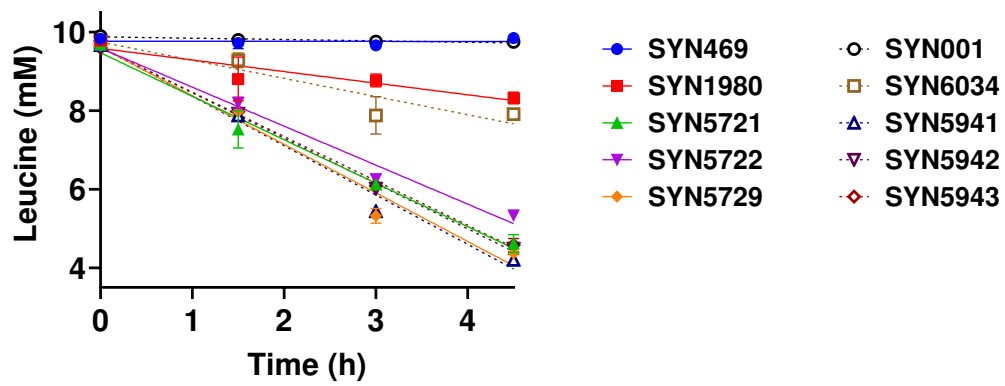


Figure 5.

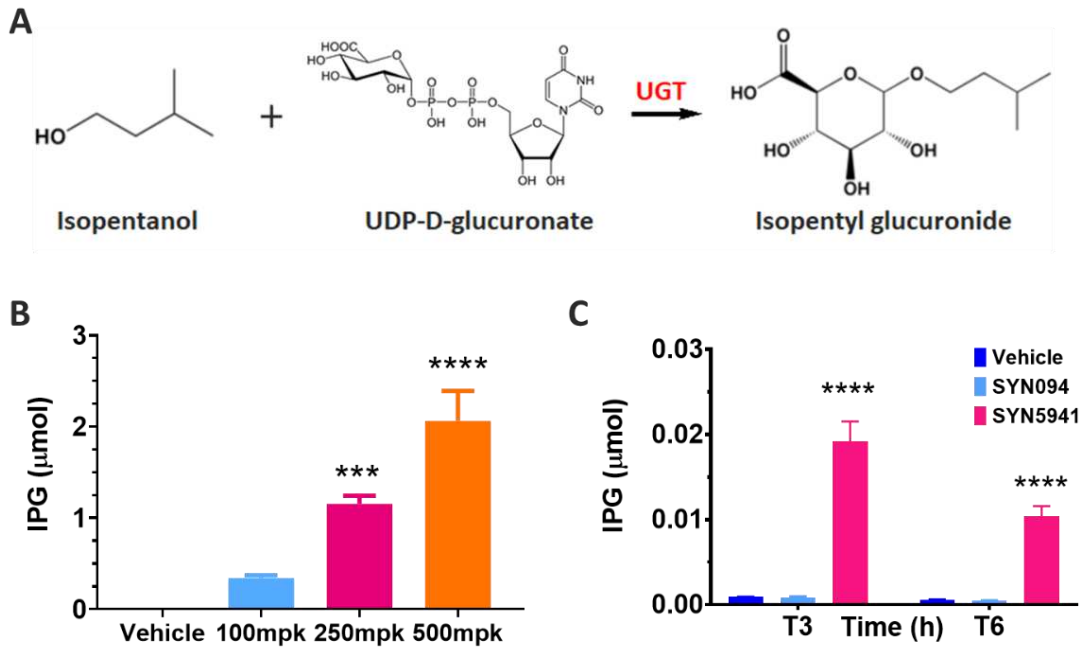
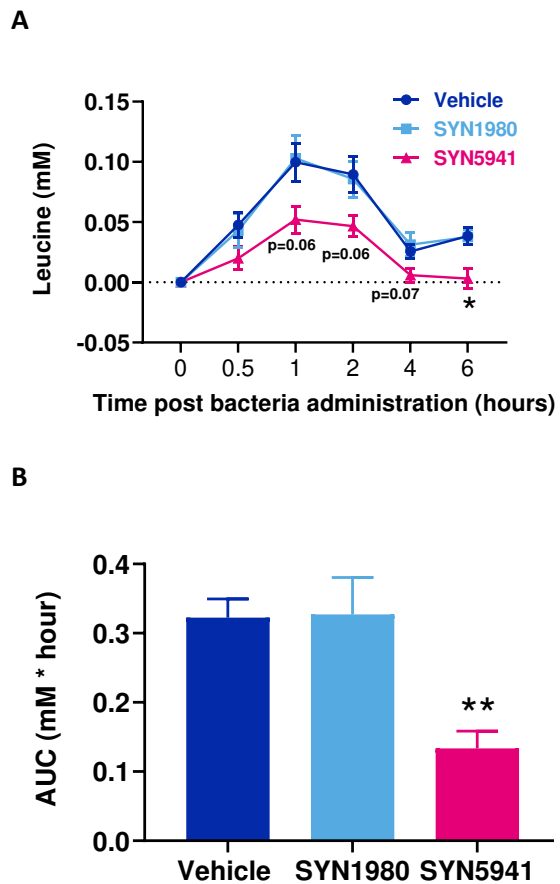
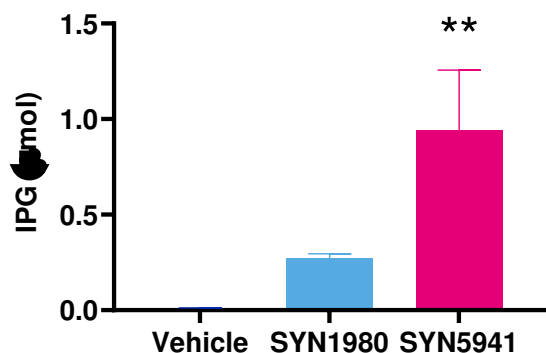


Figure 6.



c



TABLES

Table 1. Enzyme library composition

Library	Bacteria	Fungi	Animal	Plant	Total Designs
LeuDh	1129	11	23	12	1175
KivD	783	508	1	4	1296
Adh	654	273	128	122	1177

Table 2. Operon composition and leucine degradation rates of selected pathways

Strain	Rate relative to SYN1980	RBS	LeuDh source	RBS	KivD source	RBS	Adh source
SYN5721	3.8	BCD	<i>C. ceti</i> LeuDh	BCD	<i>E. iniecta</i> KivD	BCD	<i>A. dieselolei</i> Adh
SYN5722	3.7	RBS TIR=50,000 au	<i>C. ceti</i> LeuDh	RBS TIR=50,000 au	<i>E. iniecta</i> KivD	RBS TIR=5,000 au	<i>R. bacterium</i> NRL2 Adh
SYN5729	2.5	BCD	<i>C. ceti</i> LeuDh	BCD	<i>E. iniecta</i> KivD	BCD	<i>R. bacterium</i> NRL2 Adh

Supporting Information

Figures

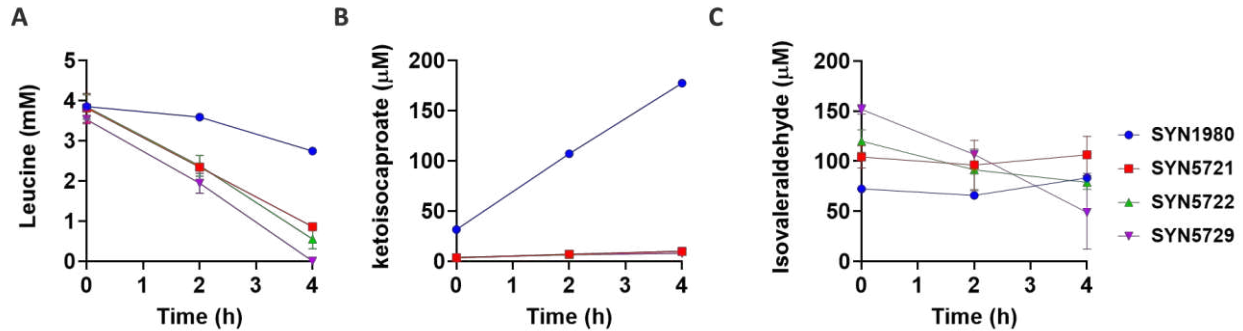


Figure S1. Intermediate analysis of leucine consuming strains. To better understand the difference between prototype strain SYN1980 and the improved strains SYN5721, SYN5722 and SYN5729, standard *in vitro* assay was performed where substrate leucine **A**), key intermediates ketoisocaproate **B**) and isovaleraldehyde **C**) were analyzed using LCMS respectively (n = 3 for each timepoint and error bar indicates standard deviation, except for SYN1980 where n = 1 for each timepoint).

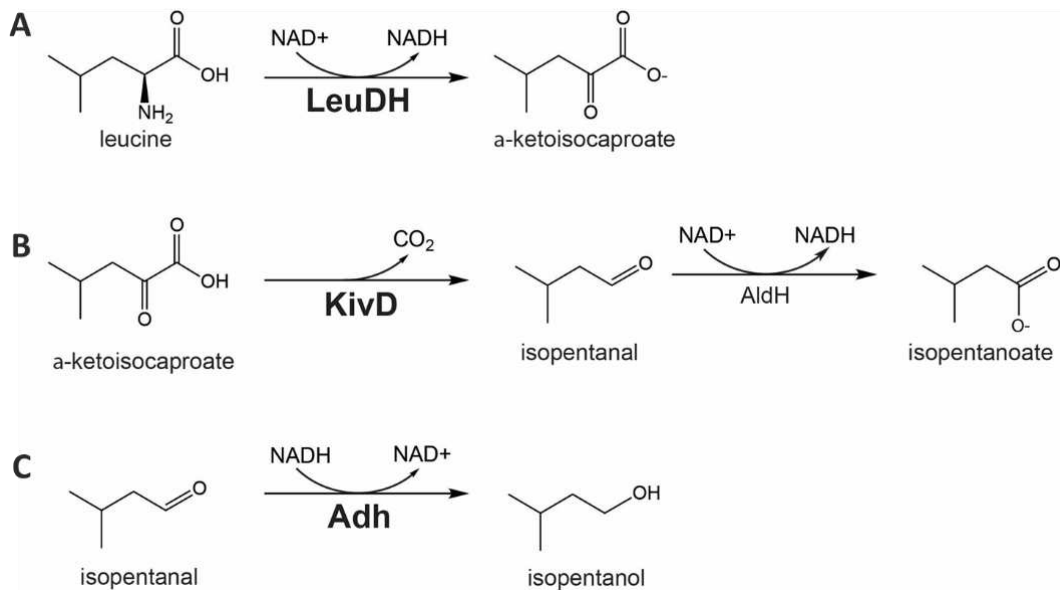


Figure S2. Enzyme activities measured in high throughput. A) LeuDH activity on leucine was measured by the reduction of NAD⁺ to NADH. **B)** An enzyme-coupled reaction was used to measure KivD activity on α-ketoisocaproate. KivD activity was indirectly measured as rate of NAD⁺-dependent oxidation of isopentanal by aldehyde dehydrogenase. **C)** Adh activity was measured by the NADH-dependent reduction of isopentanal.

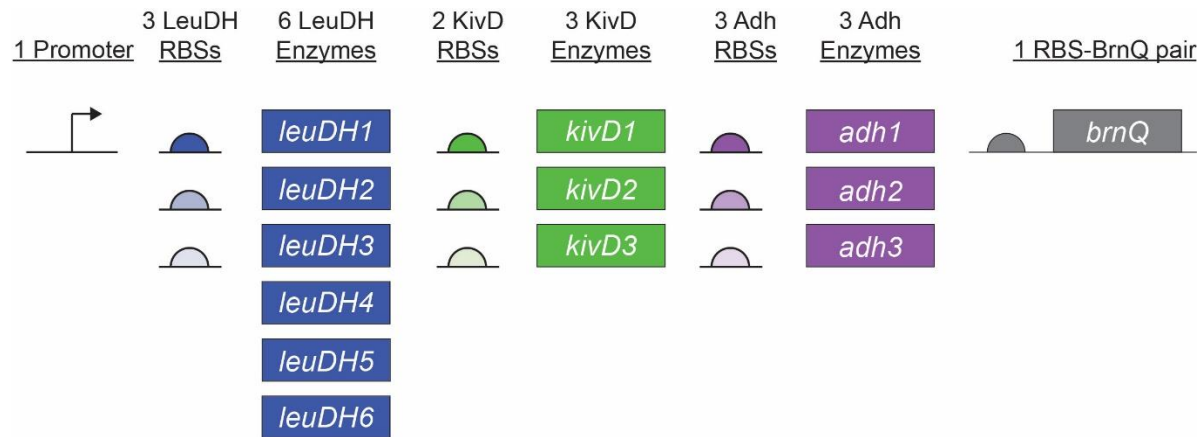


Figure S3. Combinatorial pathway design with optimized pathway enzymes. To construct the optimized pathways, each selected pathway enzyme (6 LeuDH enzymes, 3 KivD enzymes, and 3 Adh enzymes) were each paired with 3 RBSs. The RBS-enzyme pairs were combined in a partial combinatorial library, maintaining the gene order of the prototype pathway, and keeping the plasmid-encoded BrnQ intact.

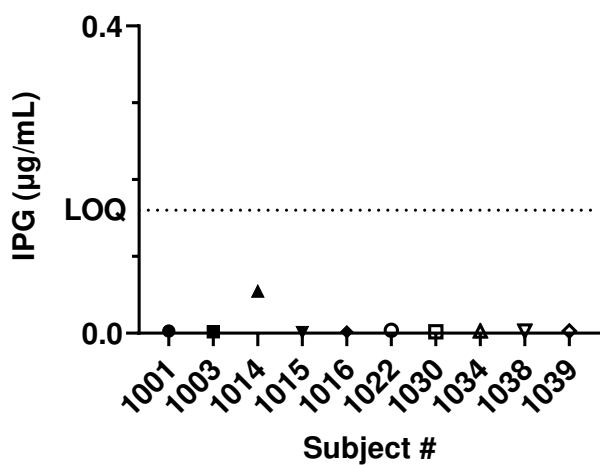


Figure S4. IPG background level in human volunteers. Urinary Isopentyl glucuronide concentration was determined from non-fasted healthy subjects. All levels were mostly zero. The limit of quantitation (LOQ) for the assay was 0.16 µg/mL.

TABLES

Table S1. List of strains used in this work

Strain	Genotype	Description
SYN001	<i>E. coli</i> Nissle 1917	Wild type bacterium
SYN094	SYN001, with strep resistance	Wild type bacterium selected for streptomycin resistance
SYN469	SYN001, $\Delta ilvC$, $\Delta leuE$, <i>lacZ::P_{tet}-livKHMPGF</i>	Bacterium with <i>ilvC</i> and <i>leuE</i> knockouts and chromosomal integration of inducible <i>livKHMPGF</i> operon
SYN1980	SYN469, pSC101-P _{tet} - <i>leuDH-kivD-adh-brnQ-ampR</i>	Bacterium with plasmid containing <i>leuDH-kivD-adh-brnQ</i> operon, <i>ilvC</i> and <i>leuE</i> knockouts and chromosomal integration of inducible <i>livKHMPGF</i> operon
SYN1992	SYN469, pSC101-P _{tet} - <i>leuDH-kivD-adh-ampR</i>	Bacterium with plasmid containing <i>leuDH-kivD-adh</i> operon, <i>ilvC</i> and <i>leuE</i> knockouts and chromosomal integration of inducible <i>livKHMPGF</i> operon
SYN5721	SYN469, pSC101-P _{tet} - <i>leuDH-kivD-adh-brnQ-ampR opt 1</i>	Bacterium with plasmid containing <i>leuDH-kivD-adh-brnQ opt1</i> operon, <i>ilvC</i> and <i>leuE</i> knockouts and chromosomal integration of inducible <i>livKHMPGF</i> operon
SYN5722	SYN469, pSC101-P _{tet} - <i>leuDH-kivD-adh-brnQ-ampR opt 2</i>	Bacterium with plasmid containing <i>leuDH-kivD-adh-brnQ opt2</i> operon, <i>ilvC</i> and <i>leuE</i> knockouts and chromosomal integration of inducible <i>livKHMPGF</i> operon
SYN5729	SYN469, pSC101-P _{tet} - <i>leuDH-kivD-adh-brnQ-ampR opt 3</i>	Bacterium with plasmid containing <i>leuDH-kivD-adh-brnQ opt3</i> operon, <i>ilvC</i> and <i>leuE</i> knockouts and chromosomal integration of inducible <i>livKHMPGF</i> operon
SYN5941	SYN001, pSC101-P _{tet} - <i>leuDH-kivD-adh-brnQ-ampR opt 1</i>	Bacterium with plasmid containing <i>leuDH-kivD-adh-brnQ opt1</i> operon,
SYN5942	SYN001, pSC101-P _{tet} - <i>leuDH-kivD-adh-brnQ-ampR opt 2</i>	Bacterium with plasmid containing <i>leuDH-kivD-adh-brnQ opt2</i> operon,
SYN5943	SYN001, pSC101-P _{tet} - <i>leuDH-kivD-adh-brnQ-ampR opt 3</i>	Bacterium with plasmid containing <i>leuDH-kivD-adh-brnQ opt3</i> operon,
SYN6034	SYN001, pSC101-P _{tet} - <i>leuDH-kivD-adh-brnQ-ampR</i>	Bacterium with plasmid containing <i>leuDH-kivD-adh-brnQ</i> operon

Table S2. LeuDH enzyme performance

LeuDH Source	Activity relative to <i>B. cereus</i> LeuDH	Protein sequence
<i>Bacillus cereus</i> (prototype)	1.0	MTLEIFEYLEKYDYEQVVFQCQDKESGLKAIHHTLGPALGGTRMWTYDSEEAIEDALRLAKGMTYK NAAAGLNLGGAKTVIIGDPRKDKSEAMFRALGRYIQGLNGRYITAEDVGTTVDDMDIHEETDFVTGISPS FGSSGNPSPVTAYGVYRGMKAAAKEAFGTDNLEGKVIQVQGVNVAHLCCKHLHAEAGKLVTDINKEA VQRAVEEFGASAVEPNEIYGVCECDIYAPCALGATVNDETIPQLKAKVIAGSANNQLKEDRHGDIHEMGI YAPDYVINAGGVINVADELGYGNRERALKRVESIYDIKAKVIEISKRDGIATVVAADRLAEERIASLKNRS TYLRNGHDIISRR-
<i>Cetobacterium ceti</i>	3.4	MNIFKMEEFNYEQLVYFYDSEITELKGITCIHNTLGPALGGTRLWNYNSEEDAVEDVIRLARGMTYKAA CAGLNLGGGKTVLIGDAKKIKSEYFRGLGRYVQSLNGRYITAEDVNTSTKDMAYVAMETDYVVLGGGK SGNPNPSPVTAYGAFMGIAKALMKKFDSSIEGRFAVQVAGQTYLLIDYLLGNKFKKAKKIKYFTEINE SYIERMKNKEHPEVEFISPKIYSLVDVFPVPCALGKIVNDKTIDEFKPIIAGTANNVLEREAHGNMLKER GILYAPDYVINAGGLINVYHELNGYNKENAILEVELIYDRLLLEIFNIADSLNISTNIAANFEAKRIKQIKSLKN NFIKR
<i>Hymenobacter daecheongensis</i> DSM 21074	2.2	MVEIKALTDTSVFGQIAEHQEQVVFCHDHETGLRAIIGIHTVLGPALGGTRMWHYASDAEALNDVLR SRGMTYKAAISGLNLGGGKAVIIGDAKTLKTEALLRKFRFVKNLNGKYITAEDVNMTTKDMYIIRMETK HYAGLPESMGSGDPSPTVAFGTYMGMKAAAKAFGSDSLAGKRIAVQGVHGVGTYLLEYLQKEGAK LVLDYYEDRALAEATRFAGAKMVLDEIYDQDVIYSPCALGATINDDTIGRLKCCQVIAGCANNQLQEN VHGPAVERGIVYAPDFLINAGGLINVYSEVVGSSRQGALNQTEKIFDITTVLNKAEQEGSHPQAAATK QAEERIASLGVKSTY
<i>Hymenobacter</i> sp. CRA2	1.9	MVEIQALPETSIFGQIADHQEQVVFCHDHETGLRAIIGIHTVLGPALGGTRMWHYATEAEALNDVLR SRGMTYKAAISGLNLGGGKAVIIGDAKTLKTEALLRKFRFVQNLNGKYITAEDVNMTTKDMYIIRMETK HYAGLPESMGSGDPSPTVAFGTYMGMKAAAKAFGSDSLAGKRIAVQGVHGVGTYLLEYLQKEGAK LVLDYYEDRALAEATRFAGAKMVLDEIYDQDVIYSPCALGATINDDTIGRLKCCQVIAGCANNQLQEN VHGPAVERGIVYAPDFLINAGGLINVYSEVVGSSRQGALNQTEKIFDITTVLNKAEQEGSHPQAAATK QAEERIASLGVKSTY
<i>Arenimonas</i> sp. SCN 70-307	1.8	MIFETISTSNHVEVYCHNKDAGLKAIIHHTVLGPALGGTRMWPYASEEALKDVLRLSRGMTYKAAV SGLNLGGGKAVIIGDPNKDKSEALFRAFGRFVNSLGGRYITAEDVGDVNDMEYVLRRETDYVTGVH HGGSGDPSPTVAFGTLMALQVFKGNEVDVGNYSYAVQGVHGVMEFVKLLRERAGKVFVTDINK DAVQRAVDEFGCEAVLDEIYDQDVIYSPCALGATINDDTIGRLKCCQVIAGCANNQLQEN VHGPAVERGIVYAPDFLINAGGLINVYSEVVGSSRQGALNQTEKIFDITTVLNKAEQEGSHPQAAATK QAEERIASLGVKSTY
<i>Peptococcaceae bacterium</i> CEB3	1.1	MTTFEYMEKYDYEQLVLCQDNTSGLKAVICIHHTLGPALGGTRMWNYSSEEDAILDALRLARGMTYKN AAAGLNLGGGKAVIIGDPRKDKSEALFRAFGRFVNSLGGRYITAEDVGTNVQDMWIMHMETKFTVTGIS SSYGASGDPSPVLTALGVYRGMKAAAKEAFGSDSLGKTVAIQGLGHVGYLAKHLTDEGAKLVTDINS EAVKRVAREFVATAVRTEEIYFVQKDIAPCALGAVINDETIPQLKCCQVIAGCANNQLKEDRHGDELYEK GILYAPDYVINAGGVINVADELGYNAERALKKVEMVYDVARVIAIAKRDHIPTYKAADRMAEERIAKIG KVSNTFLR
<i>Candidatus kapabacteria</i> sp. 59-99	1.1	MQIFDTLQSMGHEQVVLCSDKTGLRAIHDTSGLPALGGTRMWPYATDDDAITDALRLSRGMTYKA AVSGVNLGGGKAVIIGDPRKDKSEALFRAFGRFVNSLGGRYITAEDVGTNSRDMEWIRMETKYVTVGV GNGGSGDPSPTVLTALGVYRGMKAAAKEAFGSDSLGKTVAIQGLGHVGYLAKHLTDEGAKLVTDINS EAVKRVAREFVATAVRTEEIYFVQKDIAPCALGAVINDETIPQLKCCQVIAGCANNQLKEDRHGDELYEK GILYAPDYVINAGGLMNVASEVDGYNREKVMRQAEIYDITMNLNLTARERNILTIEASNAIAEERINKVRH VHGNFIGSPSIRGV

Table S3. KivD enzyme performance

KivD Source	Activity relative to assay background	Protein sequence

<i>Lactococcus lactis</i> (prototype)	1	MYTVGDYLLDRHELGEIEIFGVPDYNLQFLDQIISHKDMKWVGNANELNASYMADGYARTKKAFAFL TTFGVGLSANGLAGSYAENLPVVEIVGSPSTKVNQEGKFVHHTLADGDFKHFMMKHEPVTAAARLLT AENATVEIDRVLSALLKERKPVYINLPVDVAAAKAEKPSLPLKKENSTNSDQEILNKIQESLKNNAKPIVI TGHEIISFLEKTYTQFISKTKLPITTLNFGKSSVDEALPSFLGIYNGTLEPNLKEFVESADFILMLGVKLT DSSTGAFTHLLENKMLISLNIDEKIFNERIQNFDFESLISLLDLSEIEYKGYDKKQEDFVPSNALLSQ DRLWQAVENLTQSNETIVAEQGTSTFFGASSIFLKSXSHFIGQPLWGSIGYFPAALGSQIADKESRHLLFI GDGSLQLTVQELGLAIREKINPICFIINNDGYTVEREIHGPNQSYNDIPMMWYSKLPESFGATEDRVSVKI VRTENEVSVMKAEQADPNRMWYIELILAKEGAPKVLKMMGKLFQAEQNS
<i>Candida auris</i>	9.6	MSEITLGRYLFERLNQLQVQTFGLPGDFNLSLLDKIYEVDMRWAGNANELNAAAYADGYSRVKGLAC LVTTFGVGLSANGVGGAYAEHVGLLHVVGVPSSISOAKQLLLHHTLNGDFTVFRHMSNNISQTTAFI SDINSAPGEIDRCIREAWVHQRPVYVGLPANLVDLTVPASLLDTPIDLKKNPDPAQEEVETVLDLVDK SKNPIILVDACASRHSCRDVRRLLVDSTSFVPVFTPMGKSAVNESHPRFQGGVYVGLSEPNVKEAVENA DLVLSIGALLSDFTNGSFSYSYKTNIVEFHSDYTKIRQATFPQVQMKALNVLLEKIPSHVANYKPLPVP QRRVPSPGDKAAISOEWLWSRLLSSWFREGDIVITETGSAFQVQSYFPDNCIGISQVWGSIGFTVGA TLGAVMAAQEIDPKKRVLVFGDGSLLTVQEISTMVKWETTPYLFVLLNNDGYTIERLIHGETATYNDIQP WDNLGLLPLFKARDYETNRVATVGEIEALFNNSAFNENTKIRMVEVMLPRMDAPQNLVKQAEFSSKTNS EN
<i>Bacillus sp.</i> FJAT-18017	9.0	MTSMDNSSQQIPMGQKTVEYLFDCQKQEGITEIFGVPDYNFTLLDALQEYNGIRFYNGRNLNAGYA ADGYARIKGISALITTFVGLSATNAIAGANSEHVPIIHVIGSPPEKAQKERKLMHHTLMDGNFVFRVK YEPLTAYTTIVTADNARMEIPAARIKERRKPVYLVVADDVVAKPITGREVPASPLPASNQDKLLAAVEH VRRLLLEPARQPVILVDVKAMRFLQAVRELANTMNVPVATMMYKGTFTDETHPNYIGVYAGTFGSSSE VQSIVENSDCVAVGLVWSDTNTANFTAKLNPHNTIEVQPTKVKIAESQVYDRAADILQEMOKLDYRSQ SKPEKISFPYEEITGSSDEPLRAENYFPRFORMLKENDIVIAETGTFYQVMSQVQLPANTTYIMQGGWQS IGYATPAAYGASIAAPDRRLLFTGDGSMQLTQAEISSMLYQCKPIIFVLLNNDGYTIERLVNVEISPDEQ NYNDIPNWSYTKLAEAFGGELFTKTVRTNEELDEAITQAEQEYAEKLCLEMIAMADPMAPEYMHRIRNH KQEQQK
<i>Erwinia iniecta</i>	8.7	MSTTTVGDYLLYRLNEIGIEHLFGVPGDYNLQFLDHVIDHPQLTWWGCTNELNAAAYADGYARCRPAAA LLTTFGVGLSANGIAGSYAEYLPIVHIVGAPSLSAQQQGDLIHSLGEGDFSSFLRMSQPVVAQAALT PDNACKIEDRVLAEVLQRRPGYLLSTDVAAPAALPQSTLSLPTAPDHRVLAFAFSDAAEQMLAQAKS VSLADFLADRFVTRALAAWLQVPLPHATLLMGKGVLSQQQPGFVGTYAGAASIDSTRGAIEEAGVII GVGVRFSDTITAGFSQIDARRFIDIQPFPSRIGDRQDFHLMQAAVAALHQLCLRYQQQWISITAPSPPA LPPAAGSELSQNAFWQAMQNFIRPGDLLVADQGTAAFGAAALRPLQNCQLLVQPLWGSIGYSLPATFG AQATDERRVILIIGDGAQLTIQELSSMMRDGLKPIIFLLNNGYTVERAHGAEQRYNDIAAWNWQPLP QALSVMCPAQSWRVVETVQLTDVMKVIAASPRLSLVEVVLPAAMDVPLPLQAVSAALNQRNSS

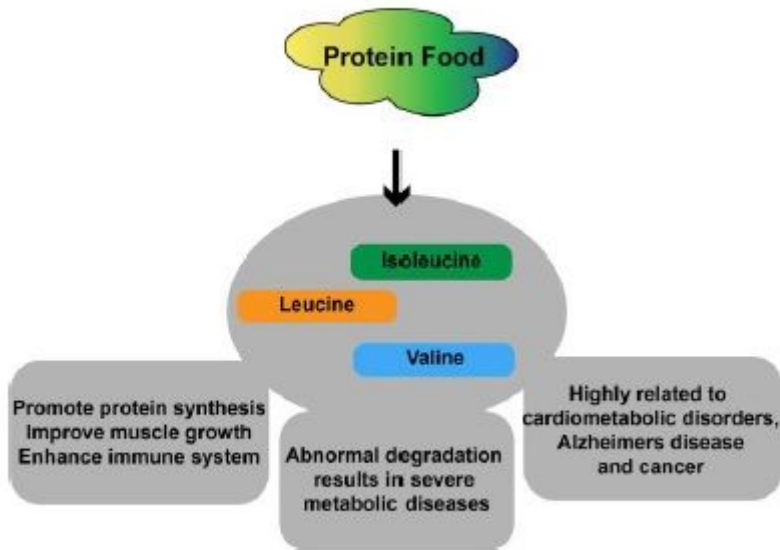
Table S4. Adh enzyme performance

Adh Source	Activity relative to assay background	Protein sequence
<i>Equus caballus</i> (positive control)	1.0	MSIPETQKAIIFYESNGKLEHKDIPVPKPKPNELLINVKYSVGVCHTDLHAWHGDWPLPTKLPLVGGHEGA GVVVMGENVKGWIKGDIYAGIKWLNKSCMACEYCELGNESNCPHADLSGYTHDGSFQEYATADAVQ AAHIPQGTDLAEVAPILCAGITVYKALKSANLRAGHWAASGAGGLGS LAVQYAKAMGYRVLIDGGP GKEELFTSLGGEVFIIDFKEDRIVSAVVKATNGGAHGIINVSVEAAIEASTRYCRANGTVVLVGLPAGAK CSSDVFNHVKISISIVGSYVGNRADTREALDFFARGLVKSPIKVVGLSSLPEIYEKMEKKGQIAGRYVVD SK
<i>Tortispora caseinolytica</i> NRRL Y-17796	12	MQTAFLYKPGHENLVRSEIPIPKAGRGEVLEIKAAGMCHSDHLVLDGGIPLPGQFVMGHEIVGTIHEIG QDVTGFKQGDLYAVHGNPNCGICTLCREGFNDCTTVAKTGQWFLGLGDGGYQKYRIPNVRISIVKVP EGVSAEAAASCTDAVLPYRALKQAGASNSTRVILGLGGLGLNALKLAKTFGSSYVYASDKPAREAA KAAGAEVLESLEPEDPLGVDIVLVVGVQSTFNLAQKHVGPRIIVPVGLASPLSNLTLALREIRVQ GTFWGTSNELAECLRLCQLGLINPKYTVVPLEEAPKYMEAMAHGKVEGRIVFHP
<i>Rhizobiales bacterium NRL2</i>	12	MRSMQFDEYGAPLKAFSYEDPTPQGKEVVRIEACGVCHSDIHLHEGYFDMGGGNKADVTRARELPFT LGHEIVGEVVATGPGVTGAKPGDKRIVYPWIGCGDCPKCNSGEDQSCARPRLNGVHVDDGGYSTHVKIP DEKFLFAYDGIPTELAGTYACSGIAYGALMKAKEAAERSGYIGLIGAGGVGMAGLMLAKAIAIGAKTVVF DIDDAKLEAATFRAGADYVFNAGAKETRKEVMKLTNGGLSGAVDFVGSKLSALFGINSALGQNGVLIIGLF GGAMTVPVPLFPLKGITVRGSYVGLSQEMSDMMELVRAGKVPMPVKTRPLDAAWETLEDLRHGKIVG RVVLTPT

	gtatgaaactaacgaatggtggccgtctgtgctgttgattcgttggcagcgataaaagcgctctgttggaaatcaacgcctgggtcagaacggcgctggtcataatggactgtogg tggcgctatgactgt tccggtacccctgttcccgctgaaaggatcacccgtacgtggctcatacgtagggtccctgcaagagatgagtgatgatggagttagttcgcgctgggaaagtccctccgatgccgtaaaaactggccactg gacgctgcctgggaaacccttgaggatclacgccatgtaaaatcgtggccgtgttctgaccccataa
--	---

Figures

A



B

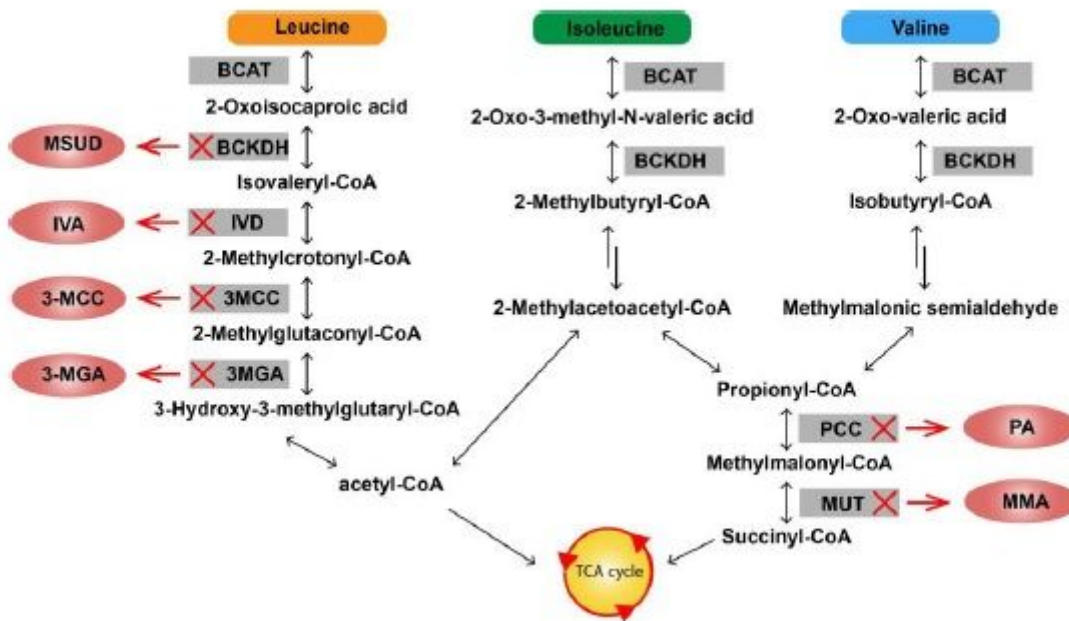


Figure 1

Branched chain amino acids and human diseases. A) Branched chain amino acids (BCAAs) are essential amino acids which humans must obtain from protein food. They benefit human health but also are believed to relate to various diseases and disorders. B) Abnormal degradation of branched chain amino acids due to defective enzymes in human will result in severe disorders such as maple syrup urine

disease (MSUD), propionic acidemia (PA), methylmalonic acidemia (MMA), isovaleryl acidemia (IVA), or 3-methylcrotonyl-CoA carboxylase deficiency (3-MCC).

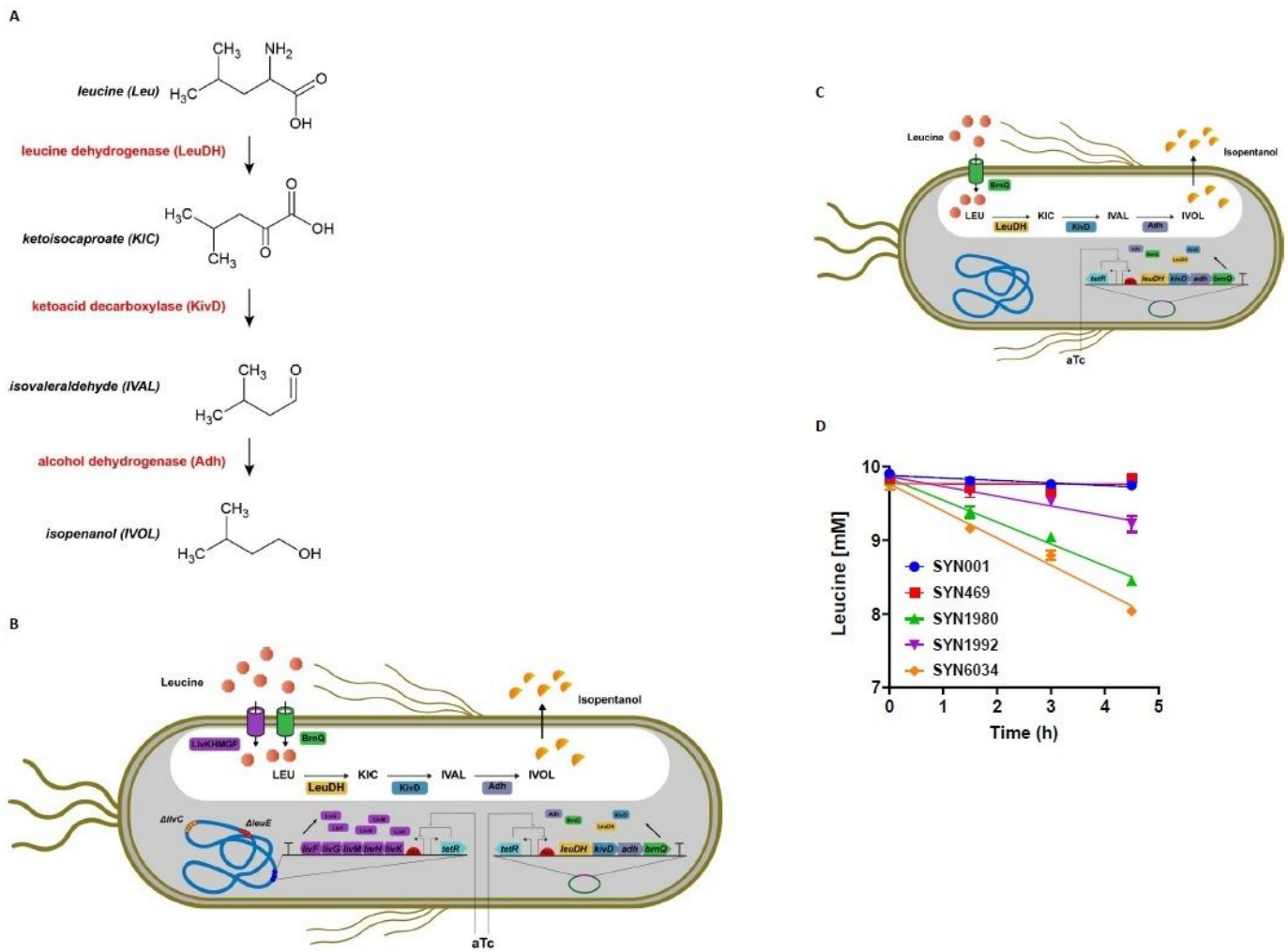


Figure 2

BCAA degradation pathway design, strain construction and in vitro activity. A) Leucine consumption pathway designed to engineer into EcN in this study. B) The scheme of prototype strain SYN1980. C) The scheme of prototype strain SYN6034. D) In vitro leucine consumption of engineered prototype strains (n = 2 for each timepoint and the error bar indicates the range of duplicates, solid lines indicate the linear regression fit of means for each strain).

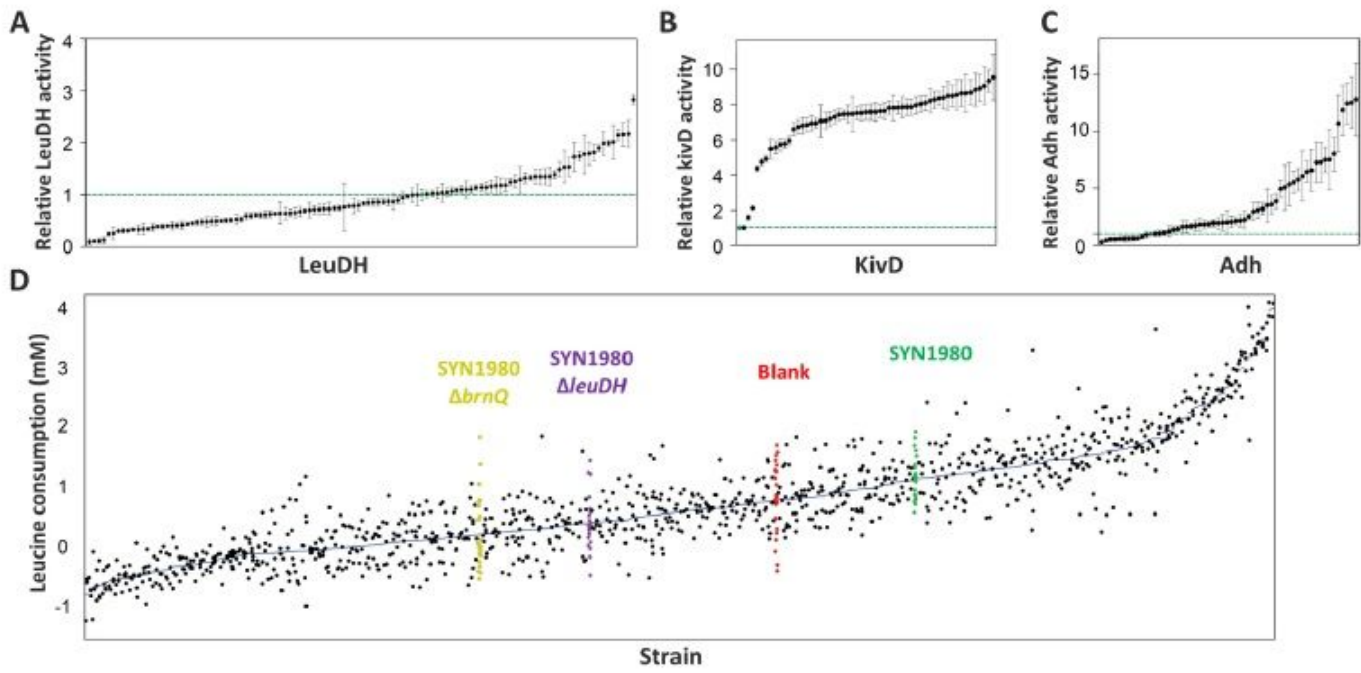


Figure 3

High throughput enzyme and operon screening results. A) The top 110 LeuDH enzymes from the primary screen were re-screened to validate enzyme activity ($n = 4$). Activities are reported as fold-improvement over the *B. cereus* LeuDH activity (green dot and green dashed line). B) The top 55 KivD enzymes from the primary screen were re-screened for activity ($n = 4$). Activities are reported as fold-improvement over of *L. lactis* KivD, which was equivalent to the non-zero assay background (green dashed line). C) Top 55 Adh enzymes from the primary screen were re-screened for activity ($n = 4$). Since the strain expressing *S. cerevisiae* ADH2 had no measurable activity in this assay, activities are reported relative to *E. caballus* Adh (green dot, green dashed line). D) Pathway operons with optimized enzymes were screened for leucine consumption. Strains were assayed in biological replicates ($n = 2$ or 3, depending on the number of successful transformants). Data points are shown as dots, and the average for each strain is shown as a horizontal blue line. Control and reference strains are indicated with colored labels.

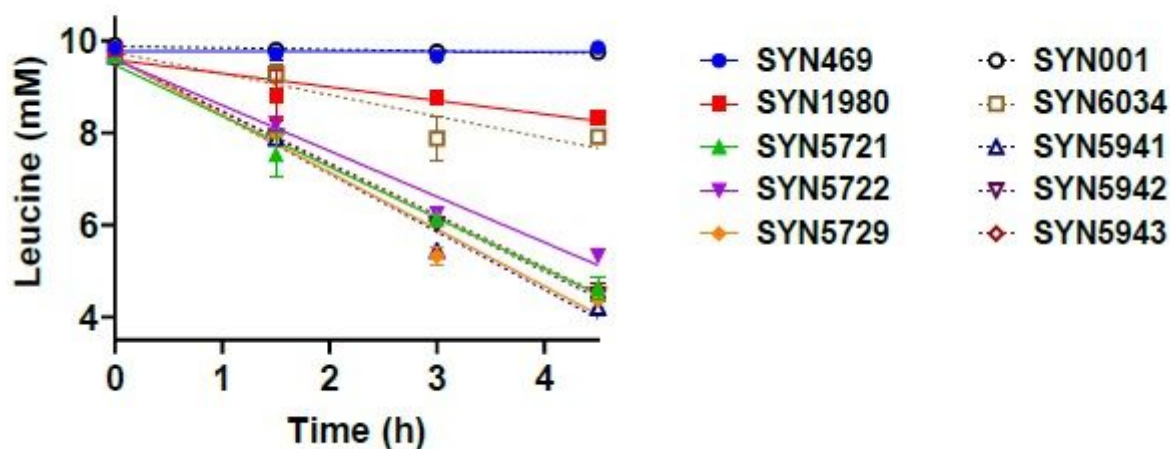


Figure 4

Confirmation of leucine consumption activity of the top strains after scaling up in fermenter. Original host strain was used as the chassis to test the activity (SYN1980, SYN5721, SYN5722, SYN5729, solid symbols with solid lines indicating the linear regression fit of means). The same four plasmids were also transformed into wild type EcN strain resulting in strains SYN6034, SYN5941, SYN5942, SYN5943). The corresponding in vitro activity was measured (empty symbols with dotted line indicating the linear regression fit of means).

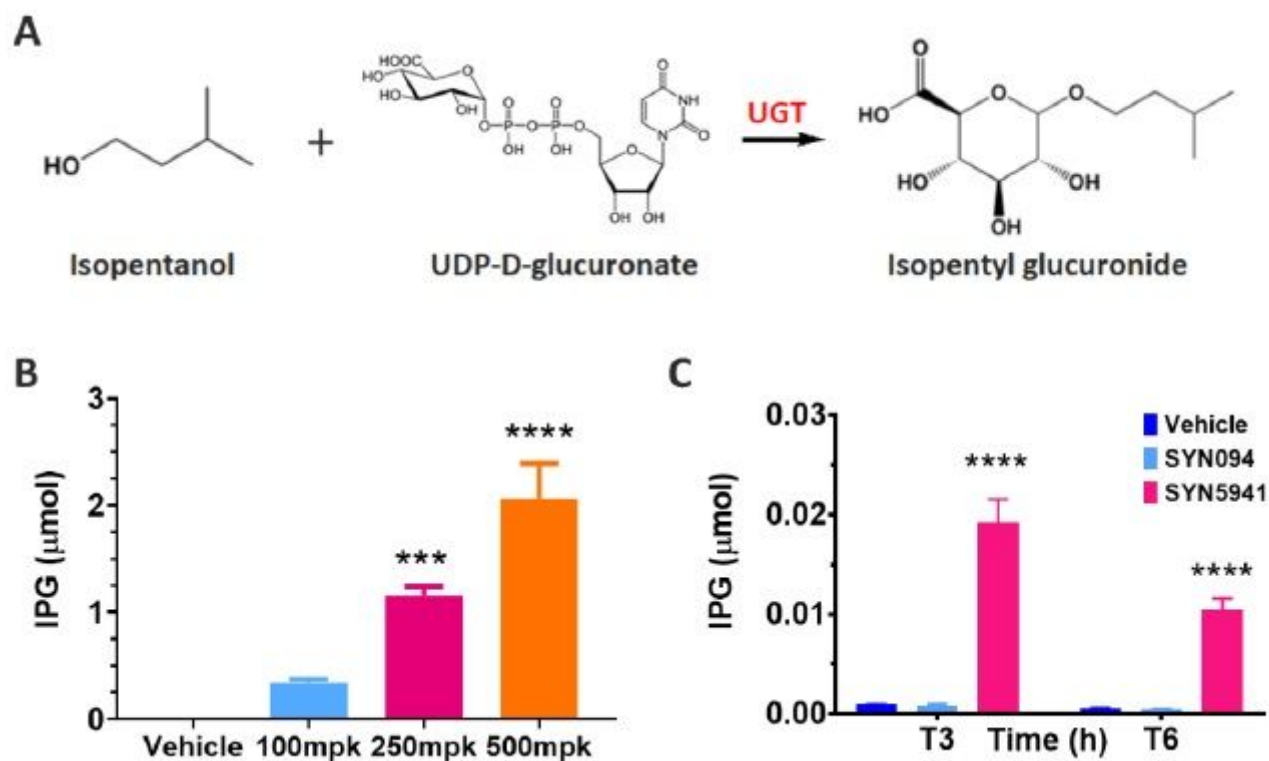


Figure 5

In vivo biomarker validation and strain activity in mice. A) Proposed pathway of in vivo isopentyl glucuronide (IPG) formation. B) IPG urinary recovery in response to oral administration of isopentanol in mice (n = 5 for each group). Statistical analysis was performed using one-way ANOVA followed by Tukey's multiple comparison test (****p < 0.0001, ***p < 0.0007 versus vehicle). C) IPG urinary recovery in response to orally administered leucine consuming strain SYN5941 in mice (n = 5 for each group, bacterial dosed at 0 h, 1 h and 2 h and totaled at 5.62 e10 cells). All vehicle & SYN094 samples are below limit of quantification = 0.00003 μ mol. Statistical analysis was performed using two-way ANOVA analysis followed by Tukey's multiple comparison test (****p < 0.0001 versus vehicle).

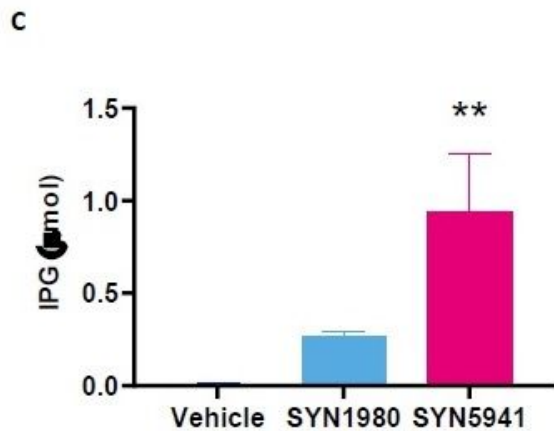
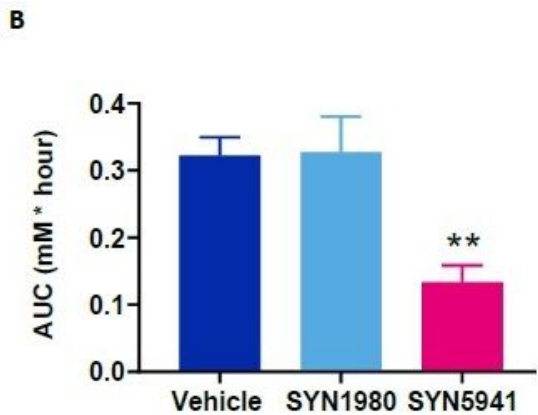
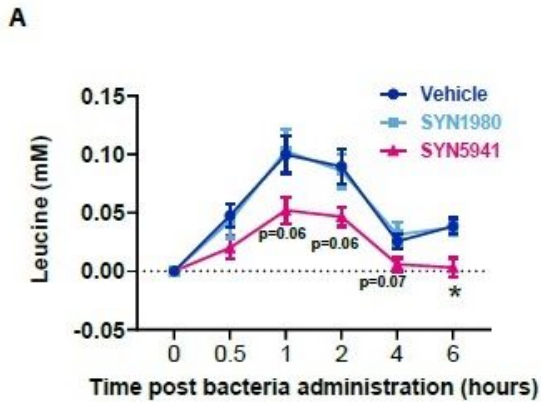


Figure 6

Efficacy of SYN1980 or SYN5941 in healthy nonhuman primates. A) Effect of SYN1980 and SYN5941 on plasma leucine levels following oral administration of leucine consuming strains. Statistical analysis was performed using two-way ANOVA analysis followed by Tukey's multiple comparison test (* $p < 0.05$ versus vehicle). B) Quantification of area under the curves (AUC) from plot A in this figure. Statistical analysis was performed using ordinary one-way ANOVA analysis (** $p < 0.0051$ versus vehicle) followed

by Tukey's multiple comparison test. C) Urinary IPG recovery following oral administration of leucine consuming strains. Statistical analysis was performed using one-way ANOVA analysis followed by Tukey's multiple comparison test (**p < 0.005 versus vehicle).